XIAP Confers Immunity Against Intracellular Bacteria

Inaugural-Dissertation

zur

Erlangung des Doktorgrades

der Mathematisch-Naturwissenschaftlichen Fakultät

der Universität zu Köln

vorgelegt von

Maria Andree

aus Nordhorn

Berichterstatter: Prof. Dr. Elena Rugarli

Prof. Dr. Rudolf Wiesner

Tag der mündlichen Prüfung: 25. Juni 2013

Table of contents

Abbreviations

BAD	BCL2 antagonist of cell death
BAX	BCL2 associated x protein
BAK	BCL2 antagonist killer 1
BCL2	B-cell lymphoma 2
BH	BCL2 homology
BID	BH3-interacting domain death antagonist
BIM	BCL2 interacting mediator of cell death
BIR	Baculovirus IAP Repeat
bp	Base pairs
BSA	Bovine serum albumin
C-	Carboxy-
Ca^{2+}	Calcium
CFU	Colony forming units
cIAP	Cellular IAP
Da, kDa	Dalton, Kilodalton
DIABLO	Direct IAP binding protein with low pI
DMSO	Dimethylsulfoxid
DTT	Dithiothreitol
EDTA	Ethylenediamine-tetraacetic acid
et al.	et alteri /-a /-um (and others)
HtrA2	Hight temperature requirement A2
IAP	Inhibitor of apoptosis
IBM	IAP-binding motif
IP	Immunoprecipitation
i.v.	*intra veneous*
M	molar, mol/l
MTS	mitochondrial targeting sequence
N-	Amino-
NF-κB	Nuclear Factor κB
MAPK	Mitogen activated protein Kinase
MOMP	Mitochondrial outer membrane permeabilization
NF-κB	Nuclear factor kappa B
PAGE	Polyacrylamid gel electro-phoresis
PBS	Phosphate buffered saline
PCR	Polymerase chain reaction
p.i.	Post infection
pmol	Picomol
PMSF	Phenylmethylsulfonyl fluoride
rpm	Revolutions per minute
RT	Room temperature
SDS	Sodium dodecylsulfate
S.f.	*Shigella flexneri*
SMAC	Second mitochondrial derived activator of caspases
STS	Staurosporine
UV	Ultra violet
WB	Western blot
XIAP	X-linked inhibitor of apoptosis

Abstract

The so-called *X-linked inhibitor of apoptosis protein* (XIAP) is the most intensively studied member of the *inhibitor of apoptosis proteins* (IAPs) and is the only cellular protein that directly binds to and inhibits caspases thereby blocking apoptosis. XIAP is frequently overexpressed in malignant cells and has therefore been investigated as a promising therapeutic target in cancer.

Recently, IAPs have also been shown to influence pathways that modulate immune signalling via activation of NF-κB. One such pathway is the NOD signalling cascade that is responsible for the detection and defence against intracellular bacteria. XIAP has previously been shown to be an essential component of the NOD signalling cascade required for the activation of NF-κB mediated inflammatory responses.

In order to study the role of XIAP in NOD signalling in response to bacterial infection, we used *Shigella flexneri* as a physiological stimulus for the NOD signalling cascade. Our data demonstrate that XIAP is essential for NF-κB activation after *S. flexneri* infection, but *S. flexneri* is able to efficiently down-regulate the XIAP-mediated inflammatory response.

In particular, we show that *S. flexneri* infection co-opts the host protease calpain to cleave the BCL2 protein BID. Calpain-cleaved BID then translocates to the mitochondria where it mediates the selective release of the XIAP-antagonists SMAC and OMI from the mitochondrial intermembrane space. In the cytosol, SMAC and OMI inhibit XIAP and therefore interrupt the NOD-mediated inflammatory response. Critically, calpain-cleaved BID induces the release of SMAC and OMI, but not of Cyt c from the mitochondria. This selective permeability differentiates this process from the mitochondrial permeabilisation induced by apoptotic stimuli and permits the infected host cell not only to survive but also ensures bacterial propagation.

The physiological importance of XIAP in controlling bacterial infection was confirmed *in vivo* in XIAP whole-body and liver-specific knockout mice, which show more bacterially induced necrotic liver lesions in response to *S. flexneri* infection than wildtype littermates. In contrast, SMAC/OMI and BID knockout mice, with unopposed XIAP activity, survived *S. flexneri* infection for much longer than wild type animals.

Our findings demonstrate how the non-apoptotic antagonisation of XIAP by mitochondrial SMAC and OMI can control the delicate interaction between intracellular microbial pathogens and their hosts.

Zusammenfassung

Das sogenannte *X-linked inhibitor of apoptosis protein* (XIAP) zählt zu den am besten untersuchten Mitgliedern der Familie der Inhibitoren der Apoptose (kurz IAPs). Bislang ist es das einzig bekannte Protein, das in der Lage ist, Caspasen direkt zu binden und zu inhibieren und somit Apoptose zu blockieren. XIAP wird in malignen Zellen häufig überexprimiert und stellt daher ein attraktives therapeutisches Ziel in der Krebstherapie dar.

In den letzten Jahren wurden IAPs zudem als Bestandteil von immunregulatorischen Signalwegen identifiziert, die meist die Aktivierung von NF-κB beinhalten. In der NOD-Signalkaskade, die für die Erkennung und Abwehr von intrazellulären Bakterien verantwortlich ist, wurde XIAP als entscheidender Faktor für die Aktivierung von NF-κB identifiziert.

Um die Funktion von XIAP im Laufe einer bakteriellen Infektion zu untersuchen, wurde das Bakterium *Shigella flexneri* als physiologischer Stimulus der NOD Signalkaskade eingesetzt. Unsere Untersuchungen zeigen, dass *S. flexneri* in der Lage ist, die XIAP-vermittelte NOD-Aktivierung zu unterdrücken. Insbesondere wurde gezeigt, dass *S. flexneri* die selektive Freisetzung der XIAP-Antagonisten SMAC und OMI aus dem mitochondrialen Intermembranraum induziert und somit XIAP inhibiert. *S. flexneri* vermittelt die Freisetzung von SMAC und OMI durch die Protease Calpain, die eine proteolytische Spaltung von BID katalysiert. Das gespaltene BID-Fragment transloziert an die Mitochondrien und induziert dort die Freisetzung von SMAC und OMI in das Cytosol. BID, prozessiert durch Calpain, permeabilisiert die Mitochondrien zwar für SMAC und OMI, jedoch ohne dabei auch Cytochrom c freizusetzen und gewährleistet somit das Überleben der infizierten Wirtszelle, um ungehinderte Vermehrung der Bakterien zu ermöglichen.

Die Bedeutung von XIAP in der Kontrolle bakterieller Infektion konnte in „XIAP knockout“ Mäusen bestätigt werden. Ganzkörper XIAP knockout- sowie leberspezifische XIAP-knockout Mäuse weisen deutlich mehr bakteriell-induzierte nekrotische Areale in der Leber auf, im Vergleich zu Wildtyp Mäusen. Im Gegensatz dazu überlebten SMAC/OMI und BID knockout Mäuse - mit ungehemmter XIAP Funktion - die *S. flexneri* Infektion deutlich länger als die Wildtyp Kontrollen. Grund hierfür ist die uneingeschränkte Funktion von XIAP, die eine bessere Bekämpfung der Infektion ermöglicht.

Zusammenfassend zeigt die vorliegende Arbeit, wie nicht-apoptotische Antagonisierung von XIAP durch mitochondriales SMAC und OMI die delikate Interaktion zwischen intrazellulären Bakterien und ihren Wirten beeinflusst.

Introduction

Inhibitor of Apoptosis Proteins (IAPs) - regulators of cell death

The *inhibitor of apoptosis proteins* (IAPs) were originally identified in baculoviruses when homologs for p35, a protein that prevents apoptosis after viral infection, were investigated. The viral CpGV gene product was found to functionally complement p35 in preventing apoptosis, caused by the *Autographa californica nuclear polyhedrosis* virus, which was thus called the *inhibitor of apoptosis* (Crook et al., 1993). One year later Clem and Miller demonstrated that IAP homologs block apoptosis independently of viral infection, indicating that IAPs interact directly with the cellular apoptotic machinery (Clem and Miller, 1994). In the following years, IAPs were found to be an evolutionary conserved protein family in various eukaryotic species including yeast, fly and mammals (Deveraux and Reed, 1999). Their defining feature is the presence of one or several zinc-finger motifs, known as *baculoviral IAP repeat* (BIR) domains (Birnbaum et al., 1994), some of which are required for their function to inhibit caspases - the main executioners of apoptosis, which is a form of programmed cell death.

The human genome encodes eight different IAPs, but in spite of their name as inhibitor of apoptosis, several members of the family are known to have distinct functions that are unrelated to apoptosis. Cellular processes such as cell cycle regulation, protein degradation and other signal transduction cascades are also subject to regulation by IAPs (Salvesen and Duckett, 2002). Nevertheless, the cellular IAPs (cIAP1 and cIAP2) efficiently impede apoptosis, triggered by multiple stimuli, when introduced into mammalian cells (Deveraux and Reed, 1999). However, cIAPs are weak caspase inhibitors, presumably lacking structural features present in other IAPs. Therefore they represent protein scaffolds suitable for direct caspase inhibition but have lost or never acquired specific caspase inhibitory interaction sites (Eckelman and Salvesen, 2006). Currently, they are widely recognised for their regulatory function in the TNF-receptor pathway (Vandenabeele and Bertrand, 2012).

The *X-linked inhibitor of apoptosis protein* (XIAP, encoded by *BIRC4*) is the best-studied IAP and the only family member that can directly bind to and inhibit caspases, thereby blocking apoptosis (Deveraux et al., 1997) (Figure 1).

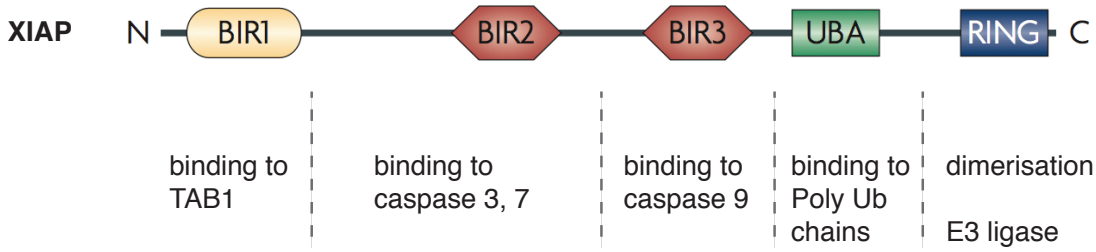

Figure 1. Domain structure of XIAP. XIAP comprises three BIR domains, each exerting different functions, a *ubiquitin-associated* (UBA) domain, which allows binding to poly-ubiquitin (Ub) chains and a RING finger domain, which is responsible for dimerisation and E3-ligase function. (modified from Gyrd-Hansen and Meier, 2010)

On the one hand, the BIR3 domain of XIAP can bind to the dimerisation surface of caspase-9, maintaining it in an inactive monomeric form. On the other hand, the linker region between the BIR1 and BIR2 domains binds to caspase-3 or -7 and blocks their activity by steric occlusion of caspase-substrates (Salvesen and Duckett, 2002). The BIR1 domain itself is not involved in caspase inactivation and interacts with a different set of proteins, implicating XIAP in other cellular functions, which will be described below.

Based on their ability to inhibit apoptosis and the frequently elevated expression of IAPs in tumour cells, IAPs have been mainly studied in mammalian cancer. Specifically, elevated expression of XIAP is often found in malignant cells and is thought to be responsible for resistance to anti-cancer therapeutics (Schimmer et al., 2006; Tamm et al., 2004a, 2004b; Mizutani et al., 2007). Congruently, ectopic overexpression of XIAP in tumour cell lines confers resistance to apoptosis (Deveraux et al., 1997) and *vice versa* XIAP-targeting by its specific knock-down sensitises tumour cells to apoptosis (Kashkar et al., 2007).

Nevertheless, XIAP-targeting has thus far failed to completely restore the apoptotic machinery under physiological conditions. Furthermore, studies assessing the prognostic importance of XIAP in tumour patients or its predictive role for chemotherapy have been inconsistent between different malignancies (reviewed in Kashkar, 2010). Additional factors such as a defective mitochondrial apoptotic pathway might be responsible for this discrepancy.

The cellular apoptotic machinery

The regulation of tissue homeostasis is critical for all multicellular organisms. The number of cells is tightly controlled by apoptosis - a form of programmed cell death (Kerr et al., 1972). Apoptosis ultimately involves the activation of caspases, members of a highly conserved

family of cystein proteases, which are responsible for the majority of proteolytic events that result in the destruction of the cell (Fuentes-Prior and Salvesen, 2004). Caspases can be activated through two major pathways: the “extrinsic” and the “intrinsic” (also called mitochondrial) pathway of apoptosis.

The extrinsic pathway of apoptosis can be initiated externally by ligands of the TNF-receptor family (e.g. TNF, FAS-ligand) that induce receptor oligomerisation and recruitment of the adaptor molecule *FAS-associated death domain protein* (FADD) to form the *death inducing signalling complex* (DISC) together with pro-caspase-8. Activated caspase-8 can then directly cleave and activate executioner caspases 3 and 7.

The intrinsic or “mitochondrial pathway of apoptosis” can be initiated autonomously by the cell and is caused by overwhelming cellular stress such as DNA damage, extensive protein aggregation or growth factor withdrawal (Strasser et al., 2000). The mitochondrial pathway of apoptosis is characterised by *mitochondrial outer membrane permeabilisation* (MOMP), which results in the release of Cytochrome c (Cyt c) from the *mitochondrial intermembrane space* (IMS). The release of Cyt c into the cytosol promotes the ATP-dependent formation of the apoptosome complex – comprising of Cyt c, *apoptotic protease-activating factor 1* (APAF-1) and pro-caspase-9 - which catalyses auto-activation of the initiator caspase-9 (Li et al., 1997; Zou et al., 1999) followed by activation of executioner caspases.

In addition, both pathways of apoptosis can intersect. Beside direct activation of executioner caspases, caspase-8-dependent cleavage of the BH3-only protein BID allows amplification of the caspase cascade to ensure efficient cell demolition (Kaufmann et al., 2012). The caspase-8-cleaved C-terminal fragment of BID (tBID) translocates to the mitochondria and leads to MOMP, followed by the release of Cyt c and downstream caspase activation. Nevertheless this step is not critical to all cell types, which are accordingly categorised into type I (BID-independent) and type II (BID-dependent) cells. Experiments with diverse cell types from BID-deficient mice have revealed an important role for BID in Fas-induced apoptosis in type II cells, which include hepatocytes and pancreatic β-cells (Yin et al., 1999; McKenzie et al., 2008). Of note, while BID knockout mice are resistant to Fas-ligand-induced hepatocyte apoptosis, additional loss of XIAP can rescue this effect. Accordingly, XIAP is one important discriminator between type I and type II Fas-induced apoptosis (Jost et al., 2009). But whether a cell behaves like type I or type II does not depend on a single determinant, but on the ratio between processed effector caspases, DISC formation, caspase-8 activation and on the levels of free XIAP, respectively (Kaufmann et al., 2012).

Apoptosis is a tightly regulated process and its dysregulation culminates in multiple human diseases. Whereas the failure to execute apoptosis in regenerating tissues contributes to cancer, excessive apoptosis in post-mitotic tissues can cause degenerative disorders. Caspases – the executioner of both apoptotic pathways - are subject to inhibition by the IAPs. IAPs therefore confer protection from death-inducing stimuli, providing an important level of control of the apoptotic pathway.

Regulators of mitochondrial outer membrane permeabilisation – the BCL2 proteins

IAP antagonisation is dependent on the liberation of mitochondrial *IAP-binding motif* (IBM)-containing proteins by MOMP. MOMP is often regarded as a point of no return and therefore must be tightly regulated. Members of the *B-cell lymphoma 2* (BCL2) family are crucial regulators of MOMP. The pro-apoptotic BCL2 members can sense cellular damage and directly induce MOMP by forming pores in the *outer mitochondrial membrane* (OMM) in contrast to the anti-apoptotic members that can block this event. The precise regulation of MOMP therefore depends on the fine-tuned interactions among pro- and anti-apoptotic BCL2 family members.

The common structural feature shared by the members of this protein family is the *BCL2 homology* (BH) domain. Functionally, BCL2 family proteins can be divided into three groups: i) anti-apoptotic members, ii) pro-apoptotic effectors and iii) pro-apoptotic BH3 only proteins (Cory and Adams, 2002) (Figure 2).

Anti-apoptotic BCL2 proteins

BCL2, BCL-W, BCL-XL, A1, MCL-1

Pro-apoptotic BCL2 proteins

Effectors

BAK, BAX, BOK

BH3-only proteins

BID, BIM, BAD, BIK, BMF, BNIP3, HRK, NOXA, PUMA

Figure 2. The BCL2 protein family. The BCL2 protein family comprises three subgroups based on their different domain structure. Anti-apoptotic members contain four conserved BH domains and one transmembrane (TM) domain. Pro-apoptotic members can be further subdivided into effectors (multi-domain proteins that cause MOMP) with three BH domains and a TM domain, while BH3-only proteins (regulators of the effectors) contain only one BH domain (modified from Tait and Green, 2010).

Anti-apoptotic BCL2 proteins, such as BCL2 itself or BCL-XL are not exclusively expressed on the OMM, but also on other cellular membranes. Nevertheless, their function has mostly been studied in the context of mitochondria where they potently inhibit apoptosis induced by cytotoxic stress. With a hydrophobic groove on their surface, anti-apoptotic BCL2 proteins can bind to pro-apoptotic family members and thus retain them in an inactive state (Sattler et al., 1997).

BAX and BAK are members of the pro-apoptotic BCL2 family and indispensable for MOMP. While individual null mutations of BAX or BAK in mice have no altered apoptotic response, BAX/BAK double null mutants show dramatically impaired apoptosis during development (Lindsten et al., 2000). Whereas BAK resides on the OMM where it is bound to anti-apoptotic MCL1 and BCL-XL (Willis et al., 2005), BAX is a soluble cytosolic monomer that undergoes conformational change upon apoptotic stimuli followed by translocation to the OMM. Once in the OMM the exposed BH3 domain of BAX binds to a hydrophobic groove of another active BAX molecule, allowing homo-oligomerisation (Dewson and Kluck, 2009). The currently held view is that during MOMP, BAX and/or BAK oligomers form pores in the OMM, that facilitate the release of Cyt c, SMAC, OMI and other soluble proteins from the IMS through a mitochondrial pore (Munoz-Pinedo et al., 2006; Youle and Strasser, 2008). However, despite decades of intensive research, the exact biochemical nature of pore formation (i.e. the number of BAX/BAK molecules required; further interaction partners) remains controversial and different models have been proposed (reviewed in Tait and Green, 2010).

The third group of BCL2 proteins, known as the “BH3-only proteins” consists of a large and diverse collection of proteins whose only common feature is the conserved BH3-domain (e.g. BID, BAD, NOXA, PUMA). They are sentinels for cellular damage and promote apoptosis either by neutralising their anti-apoptotic relatives („sensitiser“) or by directly activating BAX and BAK („direct activators“) (Chipuk et al., 2010).

Regulation of IAPs by IBM-containing proteins

Regulation of the IAPs is executed by the mitochondrial IBM-containing proteins that are released from the mitochondria following MOMP. All mammalian IBM-containing proteins that have been discovered so far, reside mainly in the IMS and need to undergo proteolytic processing to expose their IBM (Salvesen and Duckett, 2002). *Second mitochondrial derived activator of caspases* (SMAC) and OMI (also called HtrA2) are the most important IBM-containing proteins involved in apoptosis (Verhagen et al., 2000; Martins et al., 2002). SMAC and OMI are synthesised as precursor proteins in the cytosol comprising an N-terminal *mitochondrial targeting sequence* (MTS) that is cleaved off following mitochondrial import, exposing the conserved N-terminal IBM of the mature protein ("AVPI" in the case of SMAC, "AVPS" in the case of OMI). When apoptosis is initiated and MOMP occurs, SMAC and OMI are, simultaneously with Cyt c, released into the cytosol to relieve caspases from IAP inhibition (Figure 3).

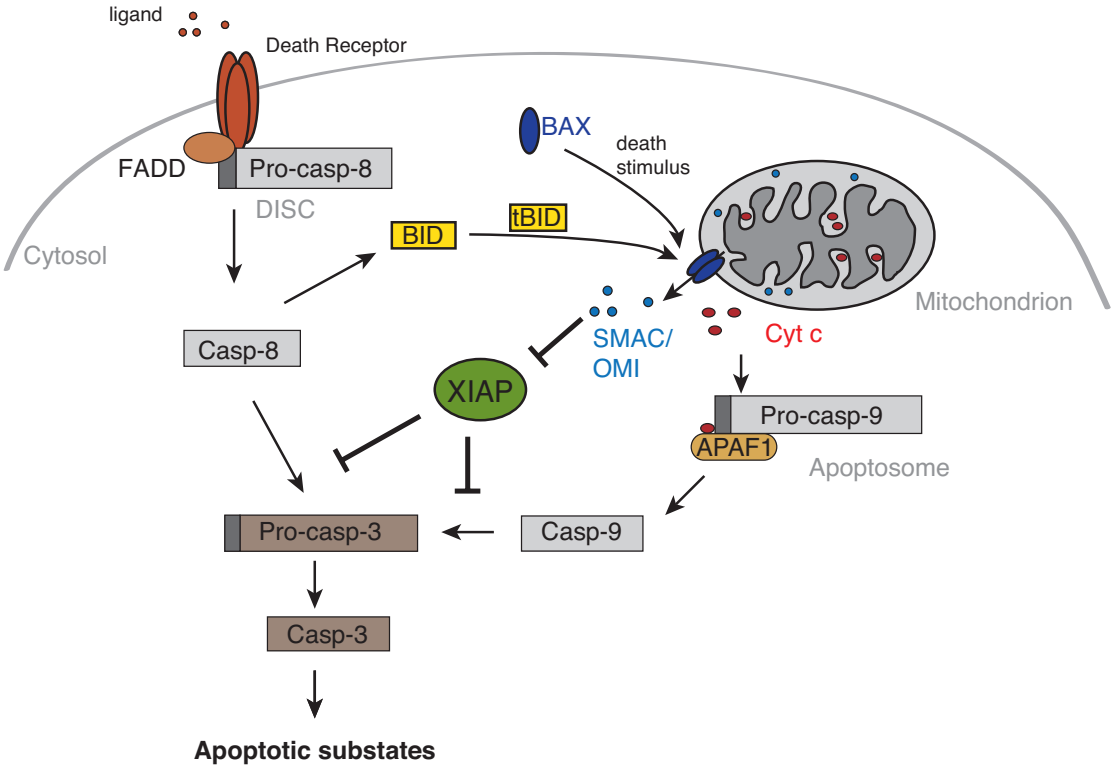

Figure 3. Extrinsic and intrinsic (mitochondrial) apoptotic pathways. Apoptosis can be induced by stimulation of death receptors with their respective ligands (TNF, FAS, TRAIL). The death receptor oligomerises and induces formation of the DISC, which activates pro-caspase-8. Active initiator caspase-8 activates executioner caspase-3 followed by cleavage of apoptotic substrates. The mitochondrial apoptotic pathway is activated upon death stimuli that lead to oligomerisation of cytosolic BAX, which inserts into the OMM and induces MOMP. SMAC, OMI and Cyt c are released into the cytosol where the latter triggers the formation of the apoptosome (together with pro-caspase-9 and APAF1), results in activation of initiator caspase-9. Caspase-9 can cleave and activate executioner caspase-3 leading to apoptotic cell death. Furthermore, SMAC and OMI antagonise XIAP,

preventing it from inactivating caspases, thus supporting the execution step of apoptosis. Caspase-8 can also activate the mitochondrial pathways of apoptosis by cleaving BID into a tBID fragment, which translocates to the mitochondria and activates BAX.

Significant efforts to develop pharmacological IAP antagonists as anti-cancer drugs have been focussing on the synthesis of the purified IAP binding motif (IBM) – that is capable of inhibiting IAPs. In recent years, several novel types of these IAP antagonists, frequently referred to as “SMAC mimetics” have entered clinical trials (LaCasse et al., 2008).

IAPs in inflammatory signalling

In addition to their well-known function in apoptosis, IAPs are increasingly being associated with diverse non-apoptotic pathways such as inflammation and innate immunity. A remarkably conserved RING finger domain equips some IAPs with E3-ligase function (Galbán and Duckett, 2010) and implicates them in ubiquitin-dependent signalling events that regulate the activation of the transcription factor *nuclear factor κB* (NF-κB) and *mitogen activated protein* (MAP) kinase pathways that drive the expression of genes involved in inflammation and cell survival (Gyrd-Hansen and Meier, 2010).

Evidence for the involvement of IAPs in innate immunity first emerged in 2005, when Gesellchen and colleagues showed that the Drosophila IAP homologue DIAP2 is indispensable for NF-κB activation in response to Gram-negative bacterial infection (Gesellchen et al., 2005).

XIAP, in particular, has been implicated in inflammatory signalling in response to intracellular bacterial infection. Specifically, XIAP knockout mice failed to clear bacterial infection with *Listeria monocytogenes* (Bauler et al., 2008) or *Chlamydophila pneumonia* (Prakash et al., 2010). It is only recently that the molecular mechanisms of XIAP in immune signalling are beginning to be understood in more detail. XIAP - and especially its E3-ligase function - was reported to be important in the NOD signalling cascade (Krieg et al., 2009; Damgaard et al., 2012). *Nucleotide-binding oligomerisation domain* (NOD) receptors are members of the *nucleotide-binding domain and leucine-rich repeat* (NLR) containing proteins that function as cytosolic pattern-recognition receptors and trigger inflammatory responses against intracellular bacteria through activation of NF-κB (Chamaillard et al., 2003). The NOD signalling pathway culminates in expression of pro-inflammatory cytokines and chemokines, necessary for a robust anti-microbial environment and proper activation of an immune response. In 2009, Krieg and colleagues proposed XIAP as a new and indispensable

component in the NOD signalling pathway in which XIAP was shown to interact with the *receptor interacting protein kinase 2* (RIPK2) via its BIR2 domain (Krieg et al., 2009). According to this view, XIAP serves as a link between the NOD signalling complex (NOD, RIPK2, XIAP) and components of the IKK-activating complex, since an interaction between XIAP and TAB1, an upstream adaptor for activation of the kinase TAK1, has been described (Lu et al., 2007). TAK1 in turn phosphorylates the catalytic subunits of the IKK complex (IKKα and IKKβ) leading to phosphorylation and proteasomal degradation of IκBs (IκBα and IκBβ). After IκB degradation, NF-κB subunits can translocate to the nucleus and activate target genes involved in the inflammatory response.

Further insight into the detailed molecular signalling pathway was recently provided by Damgaard and colleagues, who investigated the role of XIAP in NOD signalling. They provide evidence that XIAP ubiquitylates RIPK2 in response to NOD2 stimulation and thereby recruits the *linear ubiquitin chain assembly complex* (LUBAC) to the NOD signalling complex. LUBAC in turn serves as an ubiquitin ligase downstream of XIAP and is required for efficient activation of NF-κB and cytokine secretion (Damgaard et al., 2012) (Figure 4). Since NOD1 and NOD2 differ only in ligand specificity and share the majority of their signalling pathway, this finding might be relevant for NOD1 activation and needs further investigation.

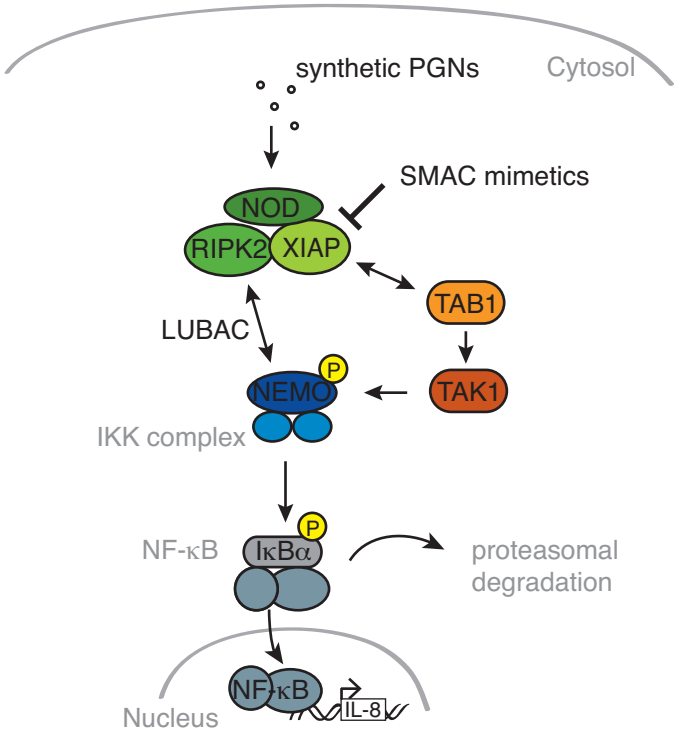

Figure 4. Intracellular NOD signalling cascade. Synthetic minimal peptidoglycan (PGN) fragments stimulate NOD, leading to complex formation with XIAP and RIPK2. Recruitment of TAB1 to poly-ubiquitylated RIPK2 activates TAK1, which in turn activates the IKK complex finally leading to proteasomal degradation of IκBα and liberation of the NF-κB subunits for nuclear translocation where

they induce expression of target genes, such as IL-8. LUBAC is recruited to polyubiquitylated RIPK2 and stabilises interaction with NEMO.

Shigella flexneri as a physiological stimulus of immune responses

The Gram-negative enteropathogenic bacterium *Shigella flexneri* represents a well-established model for intracellular infections. In patients, invasion and inflammatory destruction of the colonic epithelium by *S. flexneri* causes bacillary dysentery (Shigellosis) a severe form of bloody diarrhea, predominantly occurring in developing countries due to poor sanitary conditions.

S. flexneri is known to stimulate an innate immune response through the activation of NOD1 (Girardin et al., 2001, 2003) and is a well-suited model to analyse the complex host-pathogen interactions that shape the immune response of intestinal epithelial cells. The pathogenesis of *S. flexneri* infection is closely linked to its ability to invade and replicate in the cytosol of epithelial cells thus avoiding exposure to the extracellular host immune defence (Philpott et al., 2000). In epithelial cells an inflammatory response is produced by activation of NF-κB, followed by production of cytokines such as IL-8, leading to recruitment of immune cells to contain the bacterial infection (Phalipon and Sansonetti, 2007) (Figure 5).

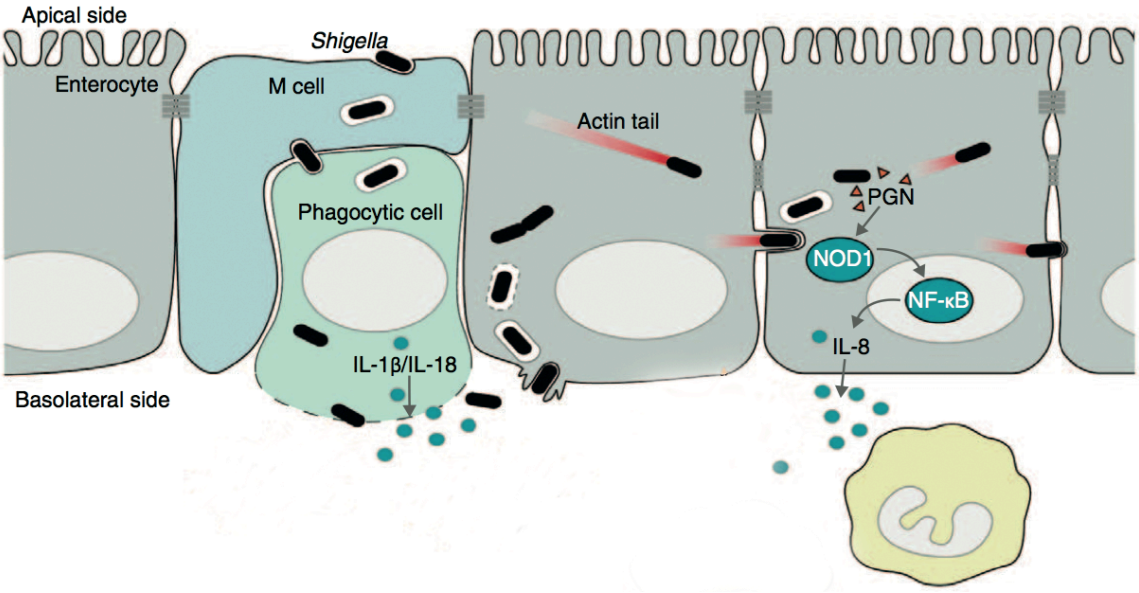

Figure 5: Infection of the colonic epithelium by *S. flexneri*. Schematic model illustrating *S. flexneri* infection of the colonic epithelium. Multiplication of *S. flexneri* in epithelial cells leads to a severe form of inflammatory colitis (Shigellosis) (modified from Ashida et al., 2011).

Aim of the study

In addition to its well-recognised function as an inhibitor of apoptosis, XIAP has recently been shown to play an important role in NOD signalling during innate immune responses (Gyrd-Hansen and Meier, 2010). Specifically, NOD signalling in response to stimulation by minimal peptidic fragments induced an inflammatory response involving NF-κB activation and cytokine release that was dependent on XIAP (Krieg et al., 2009; Damgaard et al., 2012).

However, minimal peptidic fragments are insufficient in mimicking the complex circumstances of a physiological infection and the relevance of these findings to physiological stimulation of the NOD-mediated immune responses against bacterial infection remained unresolved and is the subject of this thesis. As a natural antagonist of XIAP function, the mitochondrial intermembrane space protein SMAC is capable of disrupting XIAPs function as an inhibitor of apoptosis (Verhagen et al., 2000). On this basis we investigated whether XIAPs function in an innate immune response to bacterial infection by *S. flexneri* was similarly regulated by SMAC.

Materials and Methods

Cell Culture

The cell lines HeLa, HeLa-shXIAP, HeLa-shXIAP-mycXIAP and HeLa-shScr (Kashkar et al., 2007; Seeger et al., 2010) as well as mouse embryonic fibroblasts (MEFs) of XIAP knockout mice (gift from D. Vaux, Victoria, Australia), BID knockout mice (gift from A. Villunger, Innsbruck, Austria) and SMAC/OMI double knockout mice (gift from M. Martins, Leicester, UK) were cultured in Dulbecco's modified Eagle's medium (DMEM, Gibco (Invitrogen)) supplemented with 10% fetal calf serum (FCS, Gibco), 100 µg/ml streptomycin and 100 units/ml penicillin (Biochrom AG, Berlin, Germany).

Antibodies and reagents

All chemicals used were acquired from Roth (Karlsruhe, Germany), Sigma (München, Germany) or Merck (Darmstadt, Germany), unless indicated otherwise. Staurosporine and z-VAD-FMK were obtained from Enzo Life Sciences (Lörrach, Germany), mTNF from Genentech (San Francisco, CA, USA), tri-DAP from Invivogen (Toulouse, France) and calpain inhibitor ALLN was obtained from Calbiochem (Darmstadt, Germany).

Table 1: Primary and secondary antibodies used in western blotting

Antibody	Isotype	Supplier
β-Actin	mouse, monoclonal	Sigma (Deisenhofen, Germany)
BAD	rabbit, polyconal	Cell Signaling (Frankfurt a.M., Germany)
Bax (human)	rabbit, polyclonal	BD Bioscience (Heidelberg, Germany)
Bak	rabbit, polyclonal	BD Bioscience (Heidelberg, Germany)
BCL2 (clone 7)	mouse, monoclonal	BD Bioscience (Heidelberg, Germany)
BID	rabbit, polyclonal	BD Biosciences (Heidelberg, Germany)
BIM	rabbit, polyclonal	Cell Signaling (Frankfurt a.M., Germany)
Calpain (clone P1)	mouse, monoclonal	Millipore (Schwalbach, Germany)

Caspase 8 (1C12)	mouse, monoclonal	Cell Signaling (Frankfurt a.M., Germany)
Caspase 9	rabbit, polyclonal	Cell Signaling (Frankfurt a.M., Germany)
cIAP1	goat, polyclonal	R&D Systems (Wiesbaden, Germany)
cIAP2 (clone 315304)	mouse, monoclonal	R&D Systems (Wiesbaden, Germany)
Complex II (2E3GC12FB2AE2)	mouse, monoclonal	Invitrogen (Karlsruhe, Germany)
Cyt c (clone 7H8.2C12)	mouse, monoclonal	BD Biosciences (Heidelberg, Germany)
GFP	rabbit, polyclonal	Sigma (Deisenhofen, Germany)
FLAG (clone M2)	mouse, monoclonal	Sigma (Deisenhofen, Germany)
IκBα (C21)	rabbit, monoclonal	Santa Cruz (Heidelberg, Germany)
NOXA (114C307)	mouse, monoclonal	Calbiochen (Darmstadt, Germany)
HtrA2/Omi	rabbit, polyclonal	Cell Signaling (Frankfurt a.M., Germany)
PARP (clone C2C10)	mouse, monoclonal	BD Bioscience (Heidelberg, Germany)
RIPK2	rabbit, polyclonal	Santa Cruz (Heidelberg, Germany)
Smac/Diablo (cat. 2954)	mouse, monoclonal	Cell Signaling (Frankfurt a.M., Germany)
Smac/Diablo (mouse)	rabbit, polyclonal	Millipore (Schwalbach, Germany)
Ubiquitin (clone P4D1)	mouse, monoclonal	Cell Signaling (Frankfurt a.M., Germany)
XIAP (clone 48)	mouse, monoclonal	BD Biosciences (Heidelberg, Germany)
XIAP (2F1)	mouse, monoclonal	MBL (Eching, Germany)
Anti-mouse IgG HRP-linked	goat	Sigma (Deisenhofen, Germany)
Anti-rabbit IgG HRP-linked	goat	Sigma (Deisenhofen, Germany)
Anti-goat IgG HRP-linked	donkey	Santa Cruz (Heidelberg, Germany)

Table 2: Primary and secondary antibodies for immunofluorescence

Antibody	Isotype	Supplier
Cytochrome c Alexa Fluor 555-conjugated	mouse, monoclonal	Invitrogen (Karlsruhe, Germany)
S. flexneri serotype 5 LPS	rabbit, polyclonal	gift from P. Sansonetti (Paris, France)
Smac/Diablo (clone 7)	mouse, monoclonal	BD Bioscience (Heidelberg, Germany)
Alexa Fluor 405	goat	Invitrogen (Karlsruhe, Germany)
Alexa Fluor 488	mouse	Invitrogen (Karlsruhe, Germany)

DNA constructs

Ub-SMAC and SMACΔMTS were previously described (Kashkar et al., 2006). pUNO-IKKβ was obtained from Invivogen (Toulouse, France). RIP2-VSV was a kind gift from Margot Thome (Lausanne, Switzerland). pcDNA3.1-NOD1 was a kind gift from Gabriel Nuñez (Ann Arbor, MI, USA). FLAG-NOD1 was previously described (Kufer et al., 2006). For the construction of BID-GFP-fusion proteins, open reading frames (ORF) encoding human BID, cleaved by caspase-8 (BID_{casp8}) and BID cleaved by calpain (BID_{calp}), were amplified by PCR and cloned into pEGFP-C3 vector (Clontech, Saint-German-en-Laye, France). Primers are listed in table 3.

Table 3: Primers for DNA-constructs

Name	Sequence
BID_{casp8} forward	5' - ccc ccc aag ctt atg ggc aac cgc agc agc cac tcc c - 3'
BID_{calp} forward	5' - ccc ccc aag ctt atg aga ata gag gca gat tct gaa ag - 3'
BID reverse	5' - ccc ccc gga tcc tca gtc cat ccc att tct ggc taa gc - 3'

Bacterial infection

Bacterial infection of the indicated cells was performed using the *S. flexneri* strain M90T *afaE* as described previously (Philpott et al., 2000). M90T *afaE* is a wild-type (WT) invasive strain of *S. flexneri* serotype 5a harboring the plasmid pIL22, which encodes the afimbrial adhesin from uropathogenic *Escherichia coli* to allow better synchrony of infection (Clerc and

Sansonetti, 1987). The invasion plasmid cured strain *S. flexneri* BS176 was used as non-invasive control (both strains were kindly provided by P. Sansonetti, Paris, France). Overnight cultures of *S. flexneri* strains were diluted 1/20 in trypticase soy broth (BD Bioscience, Heidelberg, Germany) and grown to an optical density of 0.3 at 37°C. Prior to infection, cells were starved in DMEM without FCS for 1 h followed by incubation with *S. flexneri* (MOI = 30) for 15 min at RT and transferred to 37°C for 30 min (time point zero). Plates were then transferred into fresh DMEM containing 10% FCS and 50 µg/ml gentamycin to kill extracellular bacteria.

Gentamycin protection assay

Uptake of *S. flexneri* in different cell lines was analysed by lysis of pellets of infected cells in 0.5% SDS/ H_2O. Serial dilutions of cell lysates were plated onto trypticase soy broth bacto agar plates without antibiotics and incubated at 37°C for 24 h. Colonies were counted and the recovery was determined as colony forming units (cfu).

Cell viability and cell death

HeLa cells (1×10^4) were incubated in 96-well plates at 37°C in full medium and infected with *S. flexneri* at the indicated MOI and incubation time. Cell viability was assessed by the Cell Proliferation Kit II (XTT) (Roche Applied Sciences, Mannheim, Germany) according to the instructions of the manufacturer. Briefly, cells were incubated with the XTT reagents at 37°C for 4 h. The absorbance of the samples was measured with an enzyme-linked immunosorbent assay (ELISA) reader (wavelength 450 nm; reference wavelength 620 nm). The data are mean values from at least three different experiments in triplicate. Values of absorbance of untreated cells (after background subtraction) were set as 100 % viability.
Cell death was assessed by trypan blue exclusion using an automated cell counter (CountessTM, Invitrogen, Karlsruhe, Germany).

NF-κB activity

For EMSA, nuclear extracts were prepared as described (Haubert et al., 2007). Briefly, 10 µg extract were preincubated in binding buffer (5 mM Hepes, pH 7.8, 5 mM $MgCl_2$, 50 mM KCl, 0.2 mM EDTA, 0.5 mM dithiothreitol, 10% glycerol) with 500 ng of poly dI:dC (GE Healthcare, Freiburg, Germany) for 20 min at RT. NF-κB-specific radiolabelled probe

HIV-LTR (wt) 5-ATCAGGGACTTTCCGCTGGGGACTTTCCG-3 and the unrelated oligonucleotide HIV-LTR (mu) lacking the κB site 5'-GATCACTCACTTTCCGCTTGCTCACTT TCCAG-3` (1-5 x 10^4 cpm) were added and the reaction was incubated for 7 min at RT. Samples were resolved on a 6% polyacrylamide gel by electrophoreses in low ionic strength buffer (0.25x TBE). Gels were dried (Slab gel dryer, Biorad) and analysed by autoradiography.

ELISAs were performed after nuclear extraction using the TransAM® NFκB p65 Kit (Active motif, Rixensart, Belgium) according to the instructions of the manufacturer. Read out was performed on an ELISA reader (Anthos HT2) at a wavelength of 450nm/620nm.

Cell fractionation, sample preparation and Western blotting

For whole cell lysates appropriate cell numbers were incubated in CHAPS buffer on ice for 20 min followed by centrifugation at 14.000 x g for 30 min to recover the supernatant. To obtain nuclear fractions the CHAPS-pellets were resuspended in urea extraction buffer and denatured at 95°C for 5 min. For cytosolic extracts cells were incubated in HEP buffer on ice for 20 min and mechanically disrupted by repeated passage (15x) through a 26 G x ½'' needle. Mitochondria were isolated using the Mitochondria-Isolation-Kit according to the instructions of the manufacturer (Miltenyi Biotec, Bergisch Gladbach, Germany) (Hornig-Do et al., 2009). For Western blotting, equal amounts of protein were resolved by SDS-PAGE and transferred onto nitrocellulose membrane (Protran, Schleicher & Schuell) followed by incubation with the appropriate primary and secondary antibodies (table 1).

Table 4: Buffers for sample preparation and Western blotting

CHAPS lysis buffer	10 mM HEPES, pH 7.4, 150 mM NaCl, 1% CHAPS, protease complete cocktail
Urea extraction buffer	50 mM Tris (pH 6.8), 6 M urea, 3% SDS, 10% glycerol, 0.00125% bromphenol blue, 5% 2-mercaptoethanol
HEP buffer	20 mM Hepes, pH 7.5, 10 mM KCl, 1.5 mM $MgCl_2$, 1 mM EDTA, 10 µM cytochalasin B, 1 mM DTT, protease inhibitor
SDS running buffer	14.4 % (w/v) Glycin, 3 % (w/v) Tris Base, 0.1% (w/v) SDS
Laemmli sample buffer (5 x)	0,6 M Tris-HCL pH 6.8, 144 mM SDS, 25 % (v/v) Glycerol, 0.1% (w/v) Bromophenol blue, 5% (v/v) β-Mercaptoethanol
Blot transfer buffer	25 mM Tris base pH 8.3, 192 mM Glycin, 20 % (v/v)

	Methanol
Blocking buffer	10 mM Tris-HCl pH 7.4 – 7.6, 150 mM NaCl, 5 % (w/v) skim milk powder, 2 % (w/v) BSA, 0.1 % (v/v) Tween-20
Antibody dilution buffer	50 mM Tris, pH 7.6, 150 mM NaCl, 0.1% Tween-20, 5% BSA
S-PBS	1.2 M NaCl, 0.1 M NaH_2PO_4, 0.3 M K_2HPO_4, pH 7.6

Immunoprecipitation of active BAX

200 µg of whole cell lysates were brought to a final volume of 500 ml with CHAPS lysis buffer. KCl was added to a final concentration of 150 mM. Samples were incubated for 12 h at 4°C with 2 µg of monoclonal anti-Bax 6A7 antibody (BD Biosciences, Heidelberg, Germany). Antigen-antibody complexes were immobilized on GammaBind G Sepharose (GE Healthcare, Freiburg, Germany) by rotation for 2 h at 4°C. The complexes were pelleted (1 min, 14 000 x g) and the supernatant removed. The complexes were then washed three times with CHAPS/150 mM KCN and subjected to SDS-PAGE and Western blotting as described above.

RNAi interference

For siRNA mediated knock-down, HeLa cells were transfected with 200 pmol/µl siRNA using Lipofectamine™ RNAiMAX transfection reagent (Invitrogen, Karlsruhe, Germany). Cells were incubated for 48 h prior to infection with *S. flexneri*.

Table 5: siRNAs used in this work

siRNA	Sequence	Supplier
BID	sense: 5' - cuugcuccgugaugucuuutt - 3'	Ambion (Darmstadt, Germany)
BAD	sense: 5' - guacuucccucaggccuau - 3'	Ambion (Darmstadt, Germany)
BIM	sense: 5' - ccucccuacagacagagcctt - 3'	Ambion (Darmstadt, Germany)
NOXA	sense: 5' - ggugcacguuucaucaauu - 3'	Ambion (Darmstadt, Germany)
Scr	All star non targeting mix	QIAGEN (Hilden, Germany)

Caspase-3 activity

30 µg cytosolic extracts (prepared with 0.1 µM PMSF instead of protease inhibitor) were treated with increasing amounts of horse heart Cyt c as indicated and in combination with 1 mM dATP for 1 h at 30°C. For caspase-activity measurement, cytosolic extracts were filled up to a total volume of 100 µl with caspase activation buffer (20 mM Pipes, 100 mM NaCl, 1 mM EDTA, 0.1% CHAPS, 10 % sucrose, 10 mM dithiothreitol). The reaction was initiated by the addition of the fluorometric substrate 100 µM Ac-DEVD-7-amino-4-trifluoromethylcomarin (Ac-DEVD-AFC, Axxora, Lörrach, Germany), followed by readout at 400/505 nm using a Tecan GENious Pro (Tecan, Crailsheim, Germany). Caspase activity is presented as arbitrary fluorescence units per minute (FU/min); 1 FU is equivalent to 0.65 pmol released AFC.

Mitochondrial membrane potential

For analysis of mitochondrial membrane potential HeLa cells were stained with 10 µM JC-1 (Invitrogen, Karlsruhe, Germany) for 30 min at 37°C and analysed by flow cytometry. For the analysis by confocal microscopy, HeLa cells were seeded on cover slips and stained with 25 nM MitoTracker® Red CMXRos (Invitrogen) in culture media at 37°C for 30 min.

Microscopy

For immunofluorescence analyses, HeLa cells (2×10^5) were fixed with 3% paraformaldehyde, permeabilised for 30 min and blocked with blocking buffer for 30 min (table 6) Cells were incubated with the appropriate primary antibody in blocking buffer over night at 4°C. Cells were washed twice for 5 minutes with blocking buffer and incubated with secondary antibody for 1 h at room temperature. Cells were washed twice with blocking buffer and once with PBS for 5 minutes (table 2). Cover slides were mounted using Mowiol mounting medium. Imaging was performed on an UltraView VoX Spinning Disk Confocal microscope (Perkin Elmer, Rodgau, Germany) with a piezoelectric z-axis motorized stage, excited using the appropriate laser lines. For confocal images, z-axis stacks were acquired with a 60x TIRF Oil NA 1.49 objective.

For transmission electron microscopy analyses, cells were washed in phosphate buffer, fixed in fixation buffer and collected as cell pellets after centrifugation (table 6). Cell pellets were then postfixed with osmium tetroxide, and embedded in Epon (Fluka, Buchs, Switzerland).

Ultrathin sections were cut using a Leica Ultracut EM UC6 (Wetzlar, Germany) and micrographs were obtained using a Philips CM 10 transmission electron microscopy.
For phase contrast imaging, HeLa cells (2 x 10^5) were seeded onto cover slips and infected with *S. flexneri* at MOI 30. After infection cells were fixed with 3% paraformaldehyde and cover slips were mounted on microscope slides using Mowiol mounting medium. Imaging was performed on an Axioplan II fluorescence microscope (Zeiss, Jena, Germany).

Table 6: Buffers and sample preparation for microscopic analysis

Permeabilization buffer	0.1% Saponin, PBS
Blocking buffer	3% BSA, 0.1% Saponin, PBS
Mowiol	10% Mowiol, 25% Glycerol, 0.1 M Tris, 2.5% DABCO, H_2O
Phosphate buffer	0.12 M phosphate in H_2O
Fixation buffer	2% glutaraldehyde, 0.12 M phosphate buffer

Mouse strains

XIAP-deficient mice (Xiap/ICS/IR2785b/E114/2785c) were obtained from EUCOMM (The European Conditional Mouse Mutagenesis Program, ICS, Illkirch, France). For the generation of 'Knockout-first allele' XIAP knockout mice an L1L2-Bact-P cassette was inserted at position 39451542 of Chromosome X upstream of exon 3. The cassette is composed of an FRT site followed by a lacZ sequence and a loxP site. This first loxP site is followed by neomycin under the control of the human β-actin promoter, SV40 polyA, a second FRT site and a second loxP site. A third loxP site is inserted downstream of the targeted exon (exon 3) at position 39452298. Exon 3 is thus flanked by loxP sites. A "conditional ready" ($XIAP^{fl/fl}$) allele was created by crossbreeding with Flp-deleter mice (Flp recombinase expressing mice) (Dymecki, 1996). Subsequent crossbreeding with AFP-Cre mice (Kellendonk et al., 2000) resulted in a liver specific knockout mouse ($XIAP^{liver-/-}$). Like the conventional XIAP knockout mouse (Harlin et al., 2001) our XIAP knockout (Knockout-first allele) and liver specific XIAP knockout mice do not appear to have striking phenotypic defects. SMAC/OMI knockout mice (C57BL/6J background) were obtained from M. Martins (Leicester, UK) (Martins et al., 2004). BID knockout mice (C57BL/6J background) were obtained from T. Kaufmann (Bern, Switzerland) (Kaufmann et al., 2007).

Infection of mice with *S. flexneri*

Mice received food and water ad libitum. Overnight cultures of *S. flexneri* strains M90T or BS176 were prepared as described and resuspended in sterile PBS to obtain the indicated concentrations. Mice were challenged by injection of the caudal vein with the bacterial suspension. Cages were inspected every 2-3 h and deaths were recorded for 4 consecutive days or the animals were sacrificed by cervical dislocation at the desired time points. The liver was then removed, imaged with a SC 100 digital colour camera (Olympus, Hamburg, Germany) or prepared for immunohistochemical staining.

Tissue immunohistochemistry (IHC)

Livers from infected mice were fixed in 4% paraformaldehyde over night. Whole livers were processed using an ASP300 S Tissue Processor (Leica, Wetzlar, Germany). Embedded samples were cut using a sliding microtome HM 400 (Thermo Scientific, Fisher Scientific GmbH, Schwerte, Germany) to produce 5 µm thick sections. Staining with haematoxylin/eosin (Thermo Scientific, Fisher Scientific GmbH) or mouse-anti-F4+/80+ antibody (AbD serotec, Düsseldorf, Germany) was performed.

Statistical analysis

Data are presented as means of at least three independent experiments. Standard deviations were calculated as indicated in the figures legends. Two-tailed student's t-test was applied for statistical analyses. P-values for the Kaplan Meier survival curves were calculated using chi-square statistics.

Software

Plasmids	Vector NTI Suite
Grafical software	Adobe Photoshop CS4
	Adobe Illustrator CS5

Results

XIAP is required for *S. flexneri*-induced NF-κB activation

Increasing evidence implicates XIAP in immune responses, such as NOD signalling, in addition to its well-known function in apoptosis (Gyrd-Hansen and Meier, 2010). A well-studied physiological model for the activation of NOD1-mediated NF-κB signalling is the infection of cultured epithelial cells with the Gram-negative bacterium *S. flexneri* (Girardin et al., 2001). To address whether XIAP is required for the cellular immune responses towards *S. flexneri,* HeLa cell lines stably expressing a XIAP-specific short hairpin RNA (HeLa-shXIAP) or a non-targeting control shRNA (HeLa-shScr) (Figure 6A) were infected with the invasive strain *S. flexneri* M90T (in the following referred to as *S. flexneri*). XIAP knockdown resulted in markedly reduced NF-κB activation in response to *S. flexneri*, as examined by electrophoretic mobility shift assay (EMSA) (Figure 6B). Reintroduction of XIAP by stable overexpression of myc-tagged XIAP (lacking the 3' UTR, which targeted by the stable shRNA) in XIAP-deficient HeLa cells (HeLa-shXIAP-mycXIAP) restored NF-κB activation (Figure 6B). In contrast to *S. flexneri* infection, stimulation of Hela cells with TNF, induced NF-κB activation even in the XIAP-deficient HeLa cells (Figure 6B). Since the NOD1- and TNF-signalling cascade share the signalling pathway downstream of the IKK complex, this confirms that NF-κB signalling in general is not defective in HeLa-shXIAP cells. To exclude the possibility that different invasion rates of *S. flexneri* into the cell account for the reduction in NF-κB activation in XIAP knockdown cells, we showed that the invasion rates in the HeLa wt and HeLa-shXIAP cells were similar by performing a gentamycin protection assay (Figure 6C).

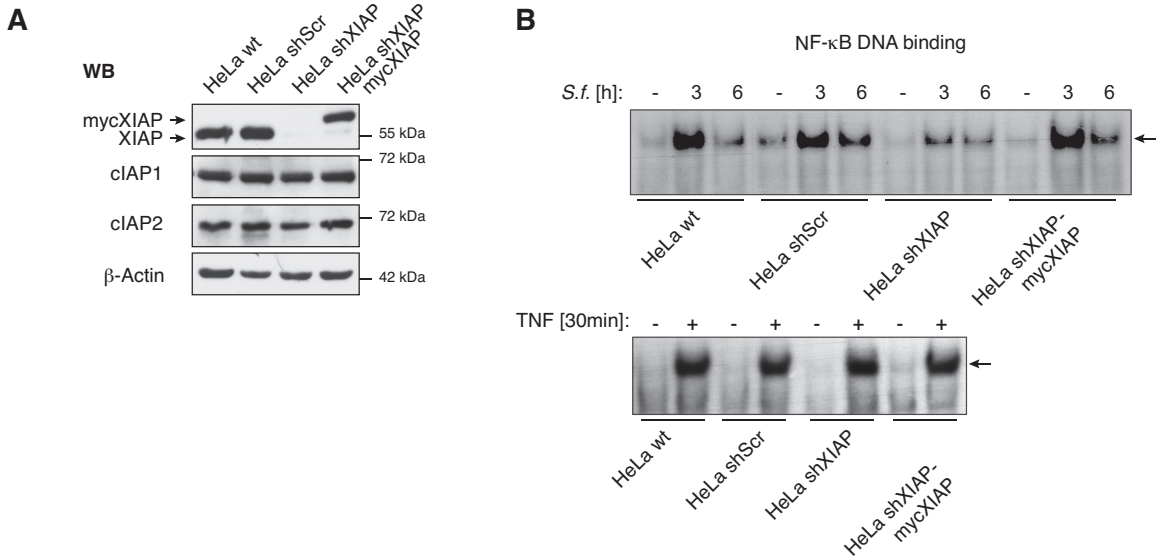

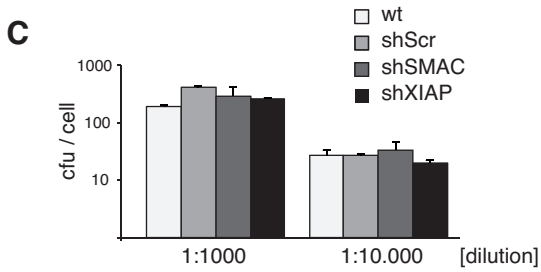

Figure 6. XIAP is required for *S. flexneri*-induced NF-κB activation in HeLa cells.
(A) Expression levels of XIAP and cIAP1/2 in HeLa wt, HeLa shScr, HeLa shXIAP (expressing shRNA targeting the 3' UTR of XIAP) and HeLa shXIAP-mycXIAP (expressing mycXIAP lacking the 3' UTR of XIAP) were analysed by Western blotting.
(B) HeLa cell lines were either left untreated (-) or were infected with *S. flexneri* M90T (*S.f.*) (MOI 30) (upper panel) or stimulated with TNF (10 ng/ml, 30 min) (lower panel). NF-κB (p65) DNA binding activity was analysed by EMSA at the indicated time points *post infection (p.i.)*.
(C) HeLa wt, HeLa shScr, HeLa shSMAC and HeLa shXIAP cells were infected with *S.flexneri* M90T (*S.f.*) (MOI 30). Cells were lysed 6 h *p.i.* and indicated dilutions were plated on trypticase soy broth bacto agar plates. Colony forming units were counted. Error bars represent mean ± SD (n=2).

In line with the data obtained in HeLa cell lines, *S. flexneri*-induced NF-κB activation was barely detectable in mouse embryonic fibroblasts (MEFs) derived from XIAP knockout mice, whereas significant NF-κB activation was observed in wild type MEFs upon infection (Figure 7A and 7B). In contrast to *S. flexneri*-induced NF-κB activation, the lack of XIAP expression did not impair TNF-induced NF-κB activation in XIAP knockout MEFs (Figure 7A, lower panel).

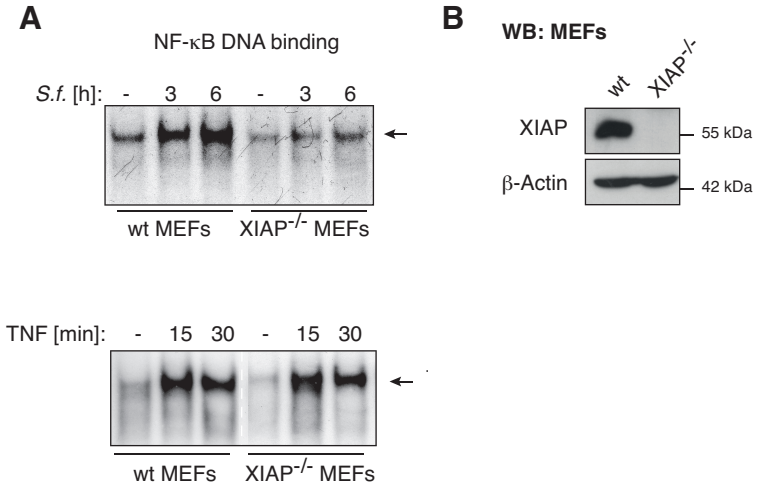

Figure 7. XIAP is required for *S. flexneri*-induced NF-κB activation in MEFs.
(A) MEFs isolated from wild type (wt) or XIAP$^{-/-}$ mice were infected with *S. flexneri* (S.f.) (MOI 30) (upper panel) or treated with TNF (10 ng/ml) (lower panel). NF-κB (p65) DNA binding activity was analysed by EMSA at the indicated time points *p.i.*.
(B) Expression levels of XIAP in XIAP$^{-/-}$ and wt MEFs were analysed by Western blotting.

Together these data identify XIAP as an indispensable component of the pro-inflammatory signalling in response to intracellular *S. flexneri*.

S. flexneri-induced release of mitochondrial SMAC interrupts NOD1/XIAP-mediated inflammatory signalling

Although the intracellular presence of *S. flexneri* potently induced NF-κB activation, NF-κB activity declined significantly 6 h post infection (*p.i.*) (Figure 6B and 7A). This was not due to the cytolytic activity of intracellular *S. flexneri* as detailed cell viability measurements failed to show any significant cell death up to 12 h *p.i.*, which was further supported by phase contrast microscopy (Figure 8A and 8B).

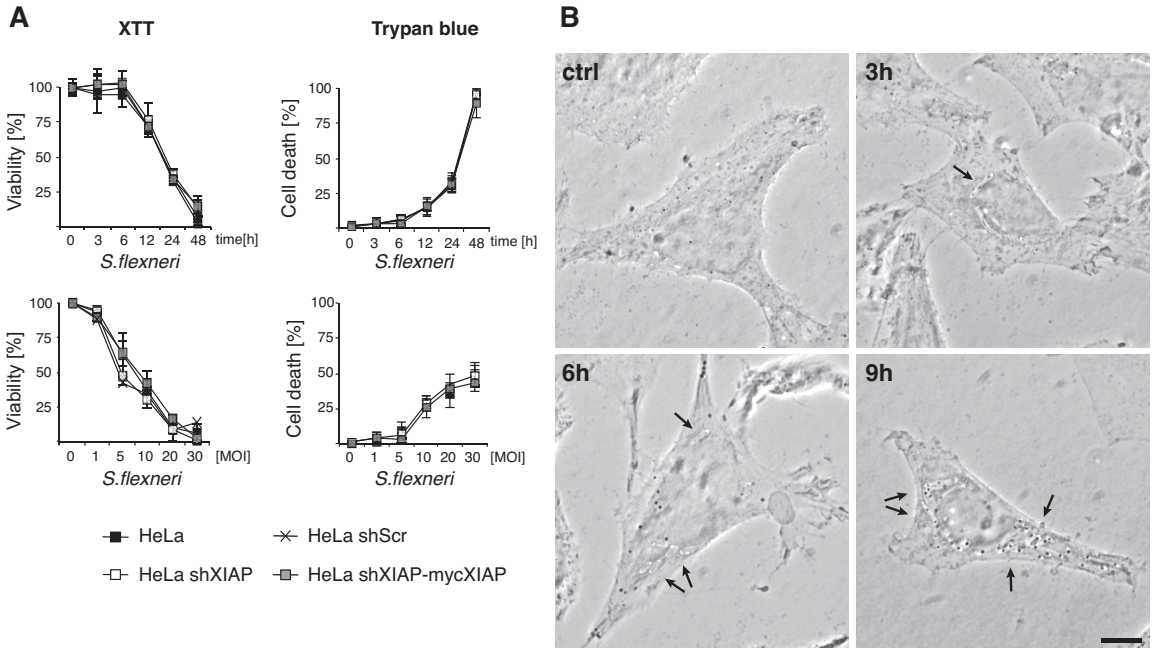

Figure 8. Cell viability is not affected upon early *S. flexneri* infection.
(**A**) HeLa wt cells were left untreated or were infected with *S.flexneri* with the indicated MOI. Cell death and cell viability were determined at the indicated time points by trypan blue exclusion (cell death) and XTT (viability). Error bars represent mean ± SD (n=3).
(**B**) HeLa wt cells were left untreated (ctrl) or were infected with *S.flexneri* (MOI 30). At the indicated time points cells were fixed and imaged by bright field microscopy. Arrows point to intracellular *S. flexneri.* (scale bar = 10 µm)

Interestingly, initial data concerning the role of XIAP in cellular immune inflammatory signalling showed that SMAC mimetics can disrupt NOD-mediated NF-κB activation in HeLa cells by antagonising XIAP (Krieg et al., 2009; Bertrand et al., 2011). However, the physiological

relevance of XIAP and its antagonisation by cellular SMAC with regard to inflammatory signalling remained unresolved. We hypothesised that inhibition of XIAP by its cellular antagonists could represent a yet unrecognised, cellular regulatory mechanism, hijacked by *S. flexneri* to escape immune detection. We therefore examined whether *S. flexneri* triggered the release of the mitochondrial XIAP antagonists, SMAC and OMI, to intercept XIAP-mediated NF-κB-activation. Detailed kinetics of *S. flexneri*-induced NF-κB activation showed a gradual decline in NF-κB activity 3 h *p.i.* (Figure 9, upper and middle panel). Western blot analysis of cytosolic fractions of infected HeLa cells revealed that SMAC and OMI accumulated in the cytosol in a time frame exactly corresponding to the decline of NF-κB activity (Figure 9, lower panel). These data suggest that *S. flexneri* is capable of usurping intracellular mechanisms to antagonise XIAP for the purpose of inhibiting NF-κB activation and preventing an anti-bacterial immune response, respectively.

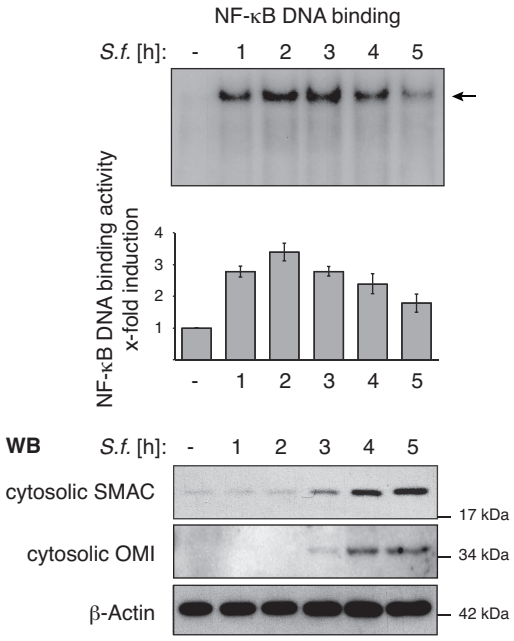

Figure 9. SMAC accumulates in the cytosol in response to *S. flexneri.*

HeLa wt cells were either left untreated (-) or infected with *S. flexneri* (*S.f.*) (MOI 30). NF-κB DNA binding activity was analysed by EMSA at the indicated time points *p.i.* (upper panel). Densitometric quantification of NF-κB DNA binding activity of five independent experiments (middle panel). Cytosolic fractions from the same experiment were analysed by Western blotting (lower panel). Error bars represent mean ± SEM (n=5)

To investigate the role of SMAC in inflammatory signalling upon *S. flexneri* infection, a stable HeLa cell line with specific knock-down of SMAC was used (HeLa-shSMAC, Figure 10B). As shown in Figure 10A, NF-κB activity (measured by EMSA and ELISA) increased within 3 h *p.i.*

and persisted through later time points in cells lacking SMAC but not in HeLa controls (HeLa-shScr). Likewise, NF-κB activation was more persistent in SMAC/OMI double knockout MEFs than in wild type MEFs (Figure 10C). These findings confirm that SMAC and OMI negatively regulate NF-κB activity after infection with *S. flexneri* by antagonisation of XIAP.

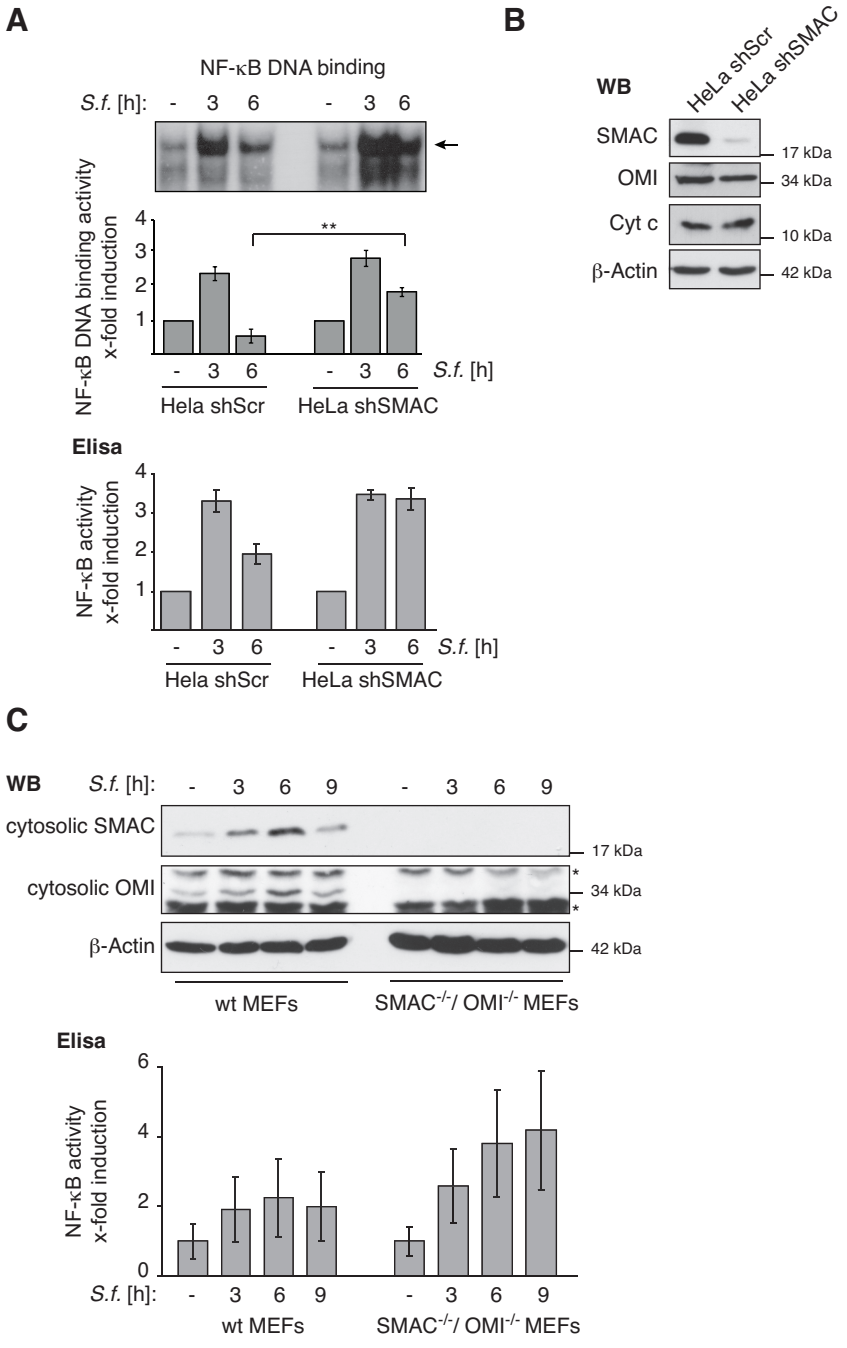

Figure 10. SMAC- and OMI-deficient cells show increased NF-κB activity upon *S. flexneri* infection.

(A) HeLa shScr or HeLa shSMAC cells were either left untreated (-) or infected with *S. flexneri* (*S.f.*) (MOI 30). NF-κB DNA binding activity was analysed by EMSA at the indicated time points *p.i.*. (upper

panel). Densitometric quantification of NF-κB DNA binding activity of five independent experiments (middle panel). NF-κB activity was analysed by ELISA (lower panel). **p <0.01
(**B**) Expression levels of SMAC, OMI and Cyt c in HeLa shScr and HeLa shSMAC cells were analysed by Western blotting.
(**C**) MEFs isolated from wild type (wt) or $SMAC^{-/-}/OMI^{-/-}$ mice were either left untreated (-) or infected with *S. flexneri* M90T (*S.f.*) (MOI 50). Cytosolic fractions were analysed by Western blotting at the indicated time points *p.i.* (upper panel, * marks unspecific band). NF-κB activity was analysed by ELISA at the indicated time points *p.i.* (lower panel). Error bars represent mean ± SEM (n=4).

Of note, unlike intracellular *S. flexneri*, activation of the NOD1 signalling cascade by overexpression of NOD1, Tri-DAP-induced activation of NOD1 or overexpression of RIPK2 did not induce the release of SMAC into the cytosol (Figure 11).

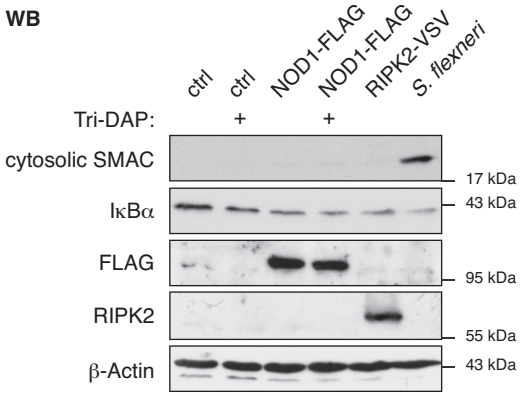

Figure 11. NOD1 activation does not induce the cytosolic accumulation of SMAC.
HeLa wt cells were either left untreated (ctrl) or transfected with expression vectors encoding NOD1-Flag or RIP2-VSV. After 24 h, cells were stimulated with Tri-DAP (10 µg/ml) (+) or were infected with *S. flexneri* (MOI 30) for 6 h. Cytosolic fractions were prepared and analysed by Western blotting.

These data suggest that *S. flexneri* employs more complex cellular mechanisms than NOD1 stimulation alone, to induce the release of mitochondrial SMAC and OMI in order to antagonise XIAP and therefore intercept the XIAP-mediated cellular inflammatory responses.

Intracellular *S. flexneri* induces the release of mitochondrial SMAC without inducing collateral cellular damage

Many enteroinvasive bacterial pathogens interfere with the cellular death machinery in order to modulate host defense mechanisms and to ensure bacterial survival and propagation (Lamkanfi and Dixit, 2010). In particular, *S. flexneri*-infected epithelial cells have been shown to remain alive during early stages of infection (Mantis et al., 1996). In line with these observations, our data show that *S. flexneri* induced the release of SMAC and OMI to intercept XIAP-mediated inflammatory response without inducing a cytotoxic effect for up to 12 h *p.i.* (Figure 8 and 9).

According to the current dogma, mitochondrial outer membrane permeabilisation involves the simultaneous release of *intermembrane space (*IMS) proteins including SMAC, OMI and Cytochrome c (Cyt c) into the cytosol where the latter then initiates the proteolytic activation of caspases to induce apoptosis. Indeed pro-apoptotic stimuli such as UV light or staurosporine (STS) induced the release of mitochondrial SMAC and OMI into the cytosol, accompanied by the co-release of Cyt c (Figure 12A, upper panel). Infection with *S. flexneri,* however, induced the release of mitochondrial SMAC and OMI, but not Cyt c, which was barely detectable in the cytosol (Figure 12A, upper panel). Without cytosolic Cyt c, *S. flexneri*-infected cells failed to activate the caspase cascade as shown by the lack of caspase-9 processing, caspase-3 activity and PARP cleavage (Figure 12A, middle panel). BAX activation has been viewed as an immediate early event preceding mitochondrial outer membrane permeabilisation in apoptotic cells (Kashkar et al., 2005). In striking contrast to apoptotic stimuli, the release of SMAC and OMI in *S. flexneri*-infected cells was not accompanied by BAX activation (Figure 12A, lower panel) suggesting that *S. flexneri* induces mitochondrial outer membrane permeabilisation in a non-apoptotic manner. These data were confirmed by confocal microscopy of *S. flexneri*-infected HeLa cells (Figure 12B). Specifically, the distribution of SMAC in infected cells was diffuse and cytosolic, whereas Cyt c-staining remained confined to a typical mitochondrial pattern 4 h *p.i.*. In contrast, in cells treated with UV light or STS, both SMAC and Cyt c appeared in the cytosol. Importantly, the accumulation of SMAC and OMI in the cytosol of *S. flexneri*-infected cells was mirrored by a reduction of SMAC and OMI in the mitochondrial fraction, whereas no significant reduction in mitochondrial Cyt c was detectable (Figure 12C).

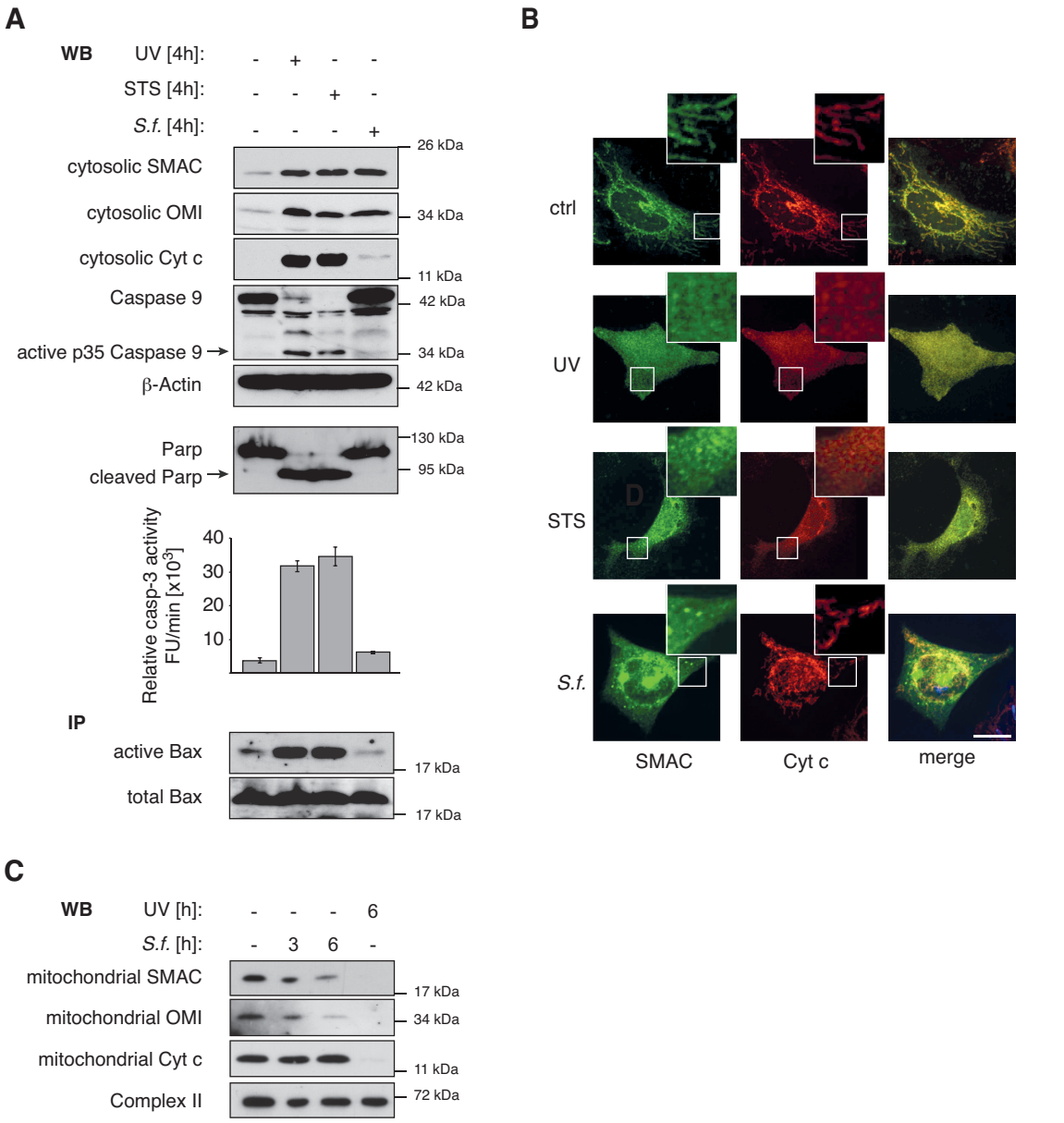

Figure 12. SMAC and OMI are selectively released from mitochondria upon *S. flexneri* infection.

(A) HeLa wt cells were either left untreated (-), treated with UV-light (10 mJ/m^2), STS (0.5 µM) or were infected with *S. flexneri* (*S.f.*) (MOI 30). After 4 h SMAC, OMI, Cyt c and caspase-9 were analysed in the cytosolic fractions by Western blotting. PARP cleavage was analysed in nuclear fractions by Western blotting. Caspase-3 activity was determined fluorimetrically in cytosolic fractions using the substrate Ac-DEVD-AFC (middle panel). Activated BAX was immunoprecipitated and analysed by Western blotting. Total amount of BAX protein was analysed in total cell lysates (lower panel). Error bars represent mean ± SEM (n=3).

(B) HeLa cells were treated as in (A). After 4 h, SMAC (green), Cyt c (red) and *S. flexneri* (blue) were stained and analysed by confocal microscopy. (scale bar = 20 µm)

(C) HeLa wt cells were treated as in (A). Mitochondria were isolated and analysed at the indicated time points by Western blotting. Complex II (flavoprotein subunit) served as a loading control.

In contrast to soluble IMS proteins including SMAC and OMI, the release of mitochondrial Cyt c requires additional biochemical or structural modifications of the mitochondrial inner membrane to mobilise the cristae-endowed Cyt c into the mitochondrial IMS and to facilitate the release of Cyt c from the mitochondrial IMS into the cytosol upon mitochondrial outer membrane permeabilisation (Martinou and Youle, 2006). Accordingly, an elevated mitochondrial membrane potential ($\Delta\Psi_m$) due to either accelerated mitochondrial respiratory activity or a pH-gradient prevents efficient Cyt c-release (Gottlieb et al., 2003). In *S. flexneri*-infected cells, Cyt c is retained in the mitochondria (Figure 12C) indicating a lack of overwhelming mitochondrial damage at early stages of infection. We therefore asked whether the $\Delta\Psi_m$ was maintained in *S. flexneri*-infected cells. In contrast to STS-treatment, which depleted the $\Delta\Psi_m$, *S. flexneri*-infection had no effect on $\Delta\Psi_m$, analysed by FACS and mitotracker staining (Figure 13A and 13B). In addition, electron micrographs showed that the cristae integrity of the inner mitochondrial membrane was preserved after infection with *S. flexneri*, but not after treatment with STS (Figure 13C). We conclude that the maintained $\Delta\Psi_m$ is responsible for the retention of Cyt c inside the mitochondria of infected cells.

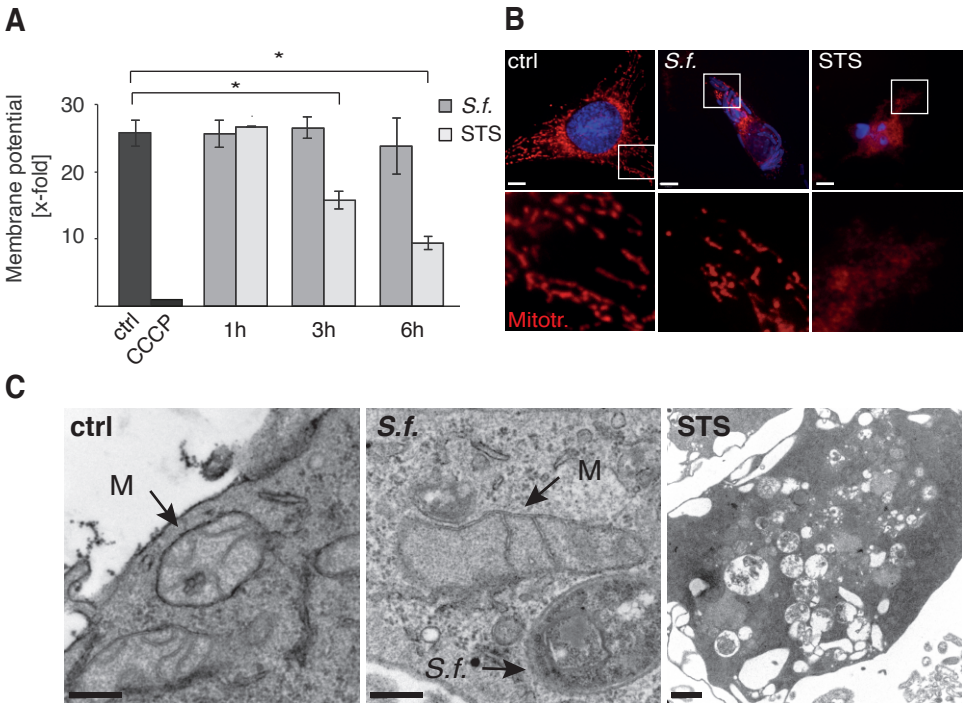

Figure 13. Mitochondria remain intact after infection with *S. flexneri*.
(**A**) HeLa wt cells were either left untreated (ctrl), infected with *S.flexneri* (*S.f.*) (MOI 30) or treated with STS (0.5 µM). $\Delta\Psi_m$ was analysed after JC-1 staining at the indicated time points using FACS analysis. CCCP was used as a reference for complete depletion of $\Delta\Psi_m$. Error bars represent mean ± SEM (n=3); *p<0.05

(**B**) HeLa wt cells were treated as in (A) and were stained with Mitotracker after 6 h. In confocal images, *S.f.* was visualized by indirect immunofluorescence (blue) and nuclei were stained with DAPI (blue). (scale bar = 8 µm).
(**C**) HeLa wt cells were treated as in (A) and mitochondrial cristae structure was analysed by transmission electron microscopy. Arrows indicate mitochondria (M) or *S. flexneri* (*S.f.*). (scale bar = 300 nm (ctrl, *S.f.*); 1 µm (STS)). Electron micrographs were performed in collaboration with Paola Martinelli.

To investigate this further, *S. flexneri*-infected cells were treated with the mitochondrial uncoupler CCCP in order to deplete $\Delta\Psi_m$ and cytosolic appearance of Cyt c was monitored by Western blotting. Upon CCCP treatment, mitochondrial Cyt c was released into the cytosol of infected cells, demonstrating the dependence of Cyt c release on $\Delta\Psi_m$ (Figure 14A). Of note, in uninfected control cells, CCCP alone did not lead to Cyt c release, indicating that in *S. flexneri*-infected cells Cyt c is merely retained in already permeabilised mitochondria by the maintenance of $\Delta\Psi_m$. The retention of Cyt c in the mitochondria likely prevents an apoptotic demise of *S. flexneri*-infected cells. Indeed, addition of recombinant Cyt c to cytosolic extracts of infected cells potently induced caspase-3 activity (Figure 14B).

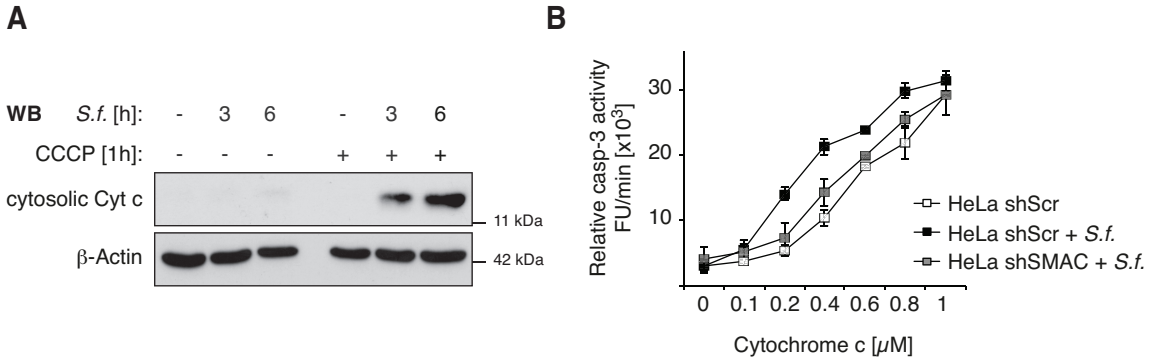

Figure 14. Cyt c released from depolarised mitochondria induces caspase activity.
(**A**) HeLa wt cells were either left untreated (-) or were infected with *S. flexneri* (*S.f.*) (MOI 30) with or without CCCP co-treatment (+) (50 µM, 1 h). Cytosolic fractions were analysed at the indicated time points by Western blotting.
(**B**) HeLa shScr and HeLa shSMAC cells were left untreated or were infected with *S. flexneri* (*S.f.*) (MOI 30) and were treated with the indicated concentrations of recombinant Cyt c. Caspase-3 activity was determined fluorimetrically in cytosolic fractions using the substrate Ac-DEVD-AFC. Error bars represent mean ± SEM (n=3). Caspase-3 activity measurement was performed by Jens Seeger.

Of note, caspase-3 activity after addition of recombinant Cyt c was more noticeable in infected than in non-infected cells, presumably caused by the cytosolic presence of SMAC in the cytosol of *S. flexneri*-infected cells, which antagonises XIAP and therefore liberates caspases from its inhibition by XIAP. Indeed, recombinant Cyt c-induced caspase activity was lower in cytosolic extracts derived from infected HeLa-shSMAC cells (Figure 14B).

Accordingly, these data suggest that *S. flexneri*-infected cells, by accumulating cytosolic SMAC are primed to undergo apoptotic cell death. This is efficiently prevented by maintaining the $\Delta\Psi_m$ that retains Cyt c inside the mitochondria.

In conclusion our data show, that the mitochondria of *S. flexneri*-infected cells, despite an overwhelming intracellular bacterial load, retain their membrane potential to ensure mitochondrial integrity and prevent apoptosis.

Calpain-cleaved BID induces the mitochondrial release of SMAC in *S. flexneri*–infected cells

In apoptotic cells the release of IMS proteins is regulated by members of the BCL2 protein family, comprised of pro- and anti-apoptotic members that are functionally controlled by a third divergent class of BH3-only proteins (Youle and Strasser, 2008). In order to investigate the regulation of *S. flexneri*-induced SMAC release, we analysed the expression and the mitochondrial association of BCL2 proteins in *S. flexneri*-infected cells (Figure 15A). The BH3-only protein BID was specifically detected in the mitochondrial fractions isolated from *S. flexneri*-infected cells, revealing a fragment significantly smaller than full-length BID. The specific detection of BID was confirmed by disappearance of the detected BID fragment after siRNA-mediated downregulation (Figure 15B).

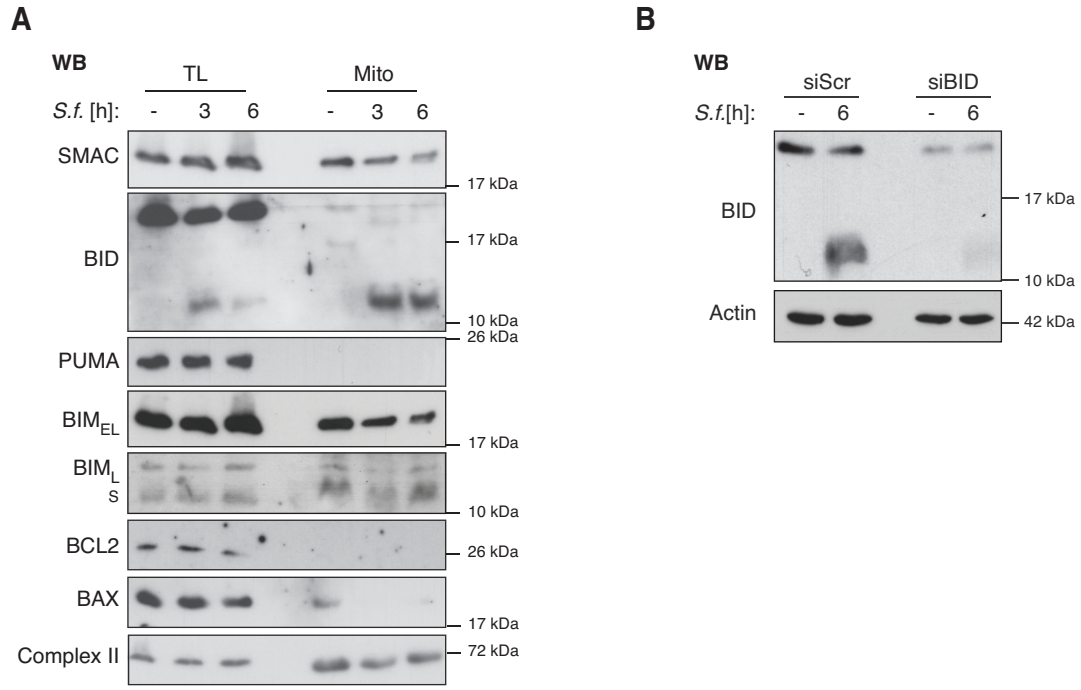

Figure 15. BID translocates to the mitochondria upon *S. flexneri* infection.
(A) HeLa wt cells were either left untreated (-) or were infected with *S. flexneri* (*S.f.*) (MOI 30). At the indicated time points total lysates and isolated mitochondria were analysed by Western blotting.

(**B**) HeLa wt cells were transiently transfected with BID-specific siRNA or non-targeting ctrl (siScr). After 48 h cells were infected with *S. flexneri* (*S.f.*) (MOI 30) for 6 h. Total lysates were analysed by Western blotting.

Interestingly, specific knockdown of BID, but not of other BH3-only proteins including BAD, BIM or NOXA, impaired the *S. flexneri*-induced release of SMAC, suggesting the involvement of BID in this process (Figure 16A). In addition, *S. flexneri* infection failed to induce SMAC release in MEFs derived from BID knockout mice (Figure 16B).

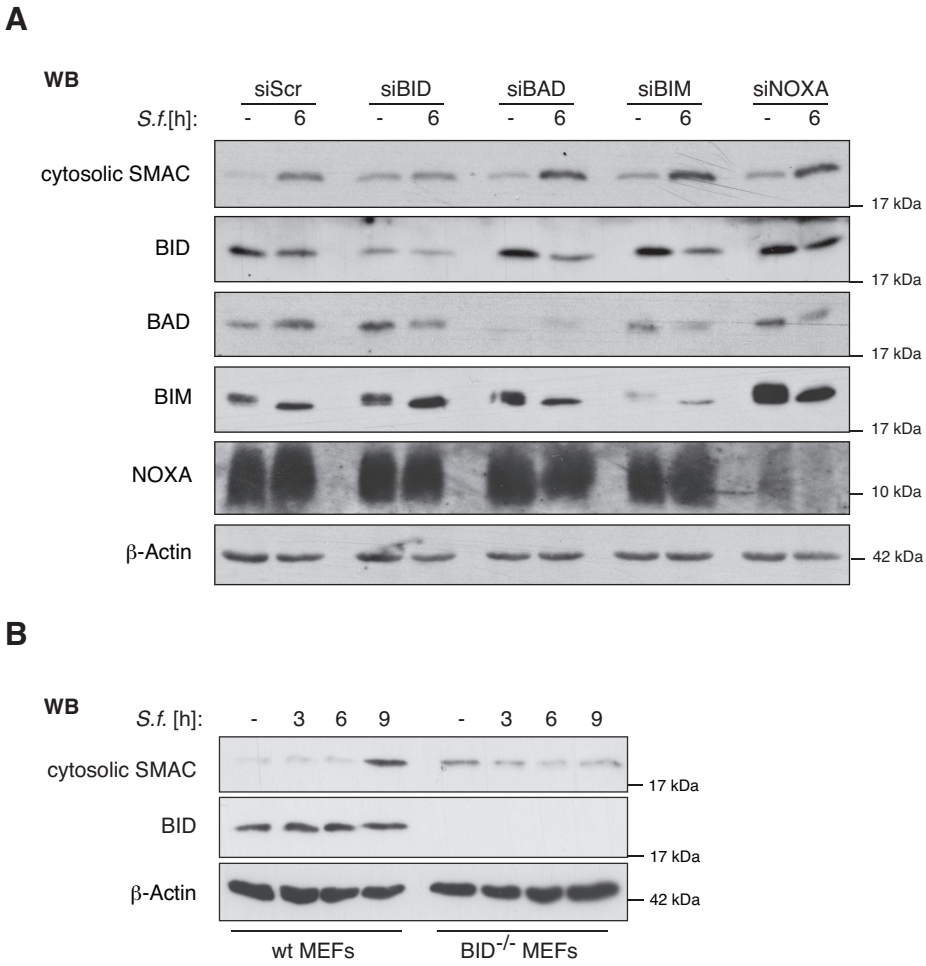

Figure 16. SMAC release is reduced in BID-deficient HeLa cells and MEFs.
(**A**) HeLa wt cells were transiently transfected with different siRNAs specific for BID, BAD, BIM, NOXA or scrambled ctrl. After 48 h cells were infected with *S. flexneri* (*S.f.*) (MOI 30) for 6 h. Cytosolic extracts and total lysates were analysed by Western blotting.
(**B**) MEFs isolated from wild type (wt) or from $BID^{-/-}$ mice were either left untreated (-) or were infected with *S. flexneri* (*S.f.*) (MOI 50). Cytosolic extracts were analysed by Western blotting at the indicated time points *p.i.*.

BID has been shown to be proteolytically processed by active caspase-8 in response to death receptor ligation (Li et al., 1998; Luo et al., 1998). Caspase-8-cleaved BID then translocates to the mitochondria where it leads to mitochondrial membrane permeabilisation through the formation of the BAX/BAK pore. However, BAX was not activated upon *S. flexneri* infection and caspase activity was not detectable (Figure 12A). Accordingly, a protease different from caspase-8 might be responsible for the proteolytic cleavage of BID in response to *S. flexneri* infection. The calpain protease has been shown to potently cleave BID (Billen et al., 2008) and calpain was recently shown to be activated by intracellular *S. flexneri* (Bergounioux et al., 2012). In line with this, we also observed calpain activation upon *S. flexneri* infection (Figure 17A). The observation that calpain can cleave BID is supported by our data that inhibition of the proteolytic activity of calpain in *S. flexneri* cells with the calpain inhibitor ALLN suppressed BID truncation (Figure 17B). Consequently, treatment of *S. flexneri*-infected cells with ALLN prevented SMAC release (Figure 17C). Of note, caspase inhibition with the pan-caspase inhibitor zVAD did not block SMAC release after *S. flexneri* infection (Figure 17C).

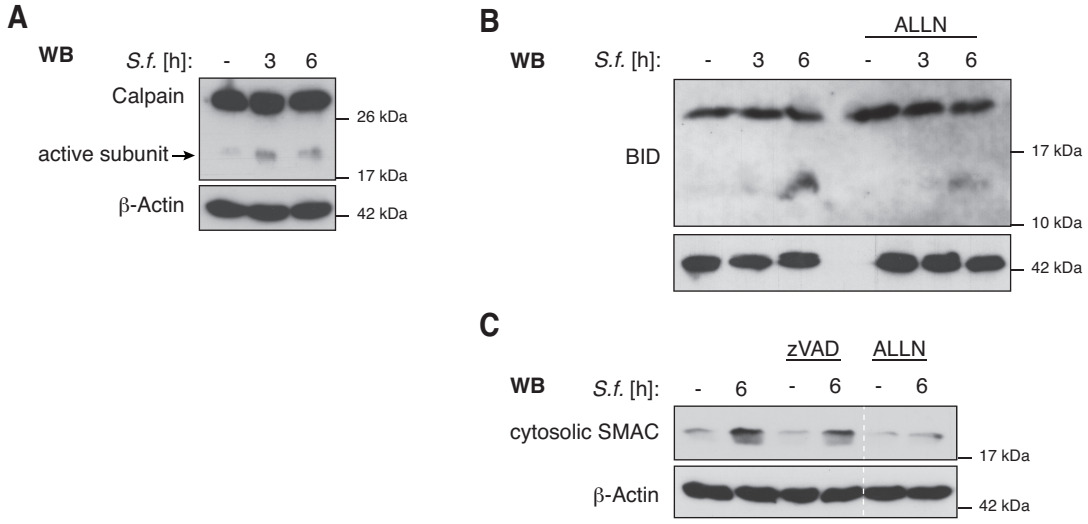

Figure 17. BID is proteolytically cleaved by calpain after *S. flexneri* infection.
(**A**) HeLa wt cells were either left untreated (-) or were infected with *S. flexneri* (*S.f.*) (MOI 30). At the indicated time points total lysates were analysed by Western blotting.
(**B**) HeLa wt cells were incubated with calpain inhibitor ALLN (1 nM). After 1 h pre-incubation, cells were infected with *S. flexneri* M90T (*S.f.*) (MOI30). Mitochondrial fractions were analysed by Western blotting at the indicated time points *p.i.*.
(**C**) HeLa wt cells were incubated with the pan-caspase inhibitor zVAD (20 µM) and the calpain inhibitor ALLN (1 nM). After 1 h pre-incubation, cells were infected with *S. flexneri* (*S.f.*) (MOI30). Cytosolic fractions were analysed by Western blotting at the indicated time points *p.i.*.

Upon proteolytic processing by caspase-8, the C-terminal fragment of BID rapidly accumulates at the mitochondria and initiates mitochondrial outer membrane permeabilisation leading to apoptotic cell death (Billen et al., 2008). In order to explore the potency of the two different BID fragments to release mitochondrial SMAC, the caspase-8 or calpain-cleaved BID fragments were ectopically expressed in HeLa cells. Both BID fragments promoted the release of similar amounts of SMAC (Figure 18). Strikingly, overexpression of caspase-8-cleaved BID (BID_{casp8}) induced Cyt c release whereas cytosolic Cyt c was barely detectable upon overexpression of calpain-cleaved BID (BID_{calp}). Accordingly, only caspase-8-cleaved BID potently induced caspase-9 activation.

In conclusion, these data indicate that *S. flexneri* infection induces calpain-dependent BID activation and identifies calpain-cleaved BID as a mediator of mitochondrial SMAC release, but not of Cyt c.

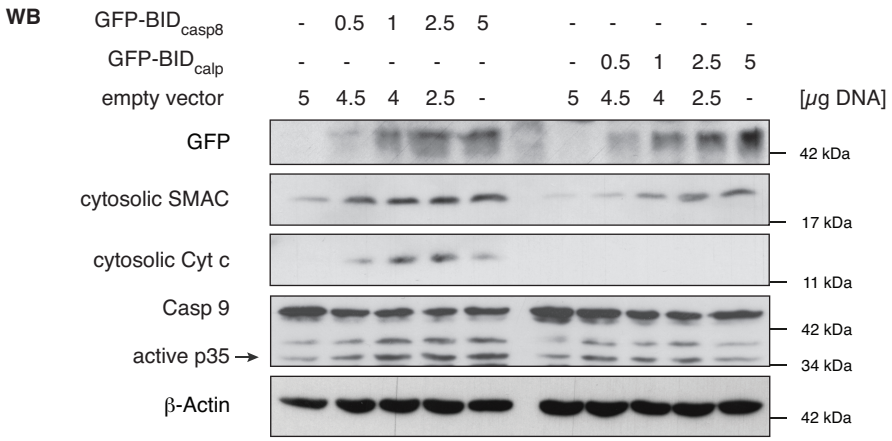

Figure 18. SMAC is selectively released upon ectopic expression of BID_{calp}.
HeLa wt cells were transiently transfected with the indicated concentrations of expression vectors encoding GFP-BID_{casp8}, GFP-BID_{calp} or empty GFP-vector. Mitochondria and cytosolic extracts were analysed by Western blotting.

XIAP confers immunity against *S. flexneri* infection *in vivo*

To investigate the physiological relevance of XIAP during anti-bacterial inflammatory responses, we employed a previously established infection model, in which intravenously injected *S. flexneri* colonise the liver of infected mice and induce the formation of microgranuloma-like lesions (Martino et al., 2005). To demonstrate that extracelluar bacterial components of *S. flexneri* are not sufficient to induce liver damage, we first showed that only the invasive strain of *S. flexneri* M90T and not the isogenic non-invasive control strain BS176 induced necrotic liver lesions associated with increased mortality upon infection in wildtype

animals at doses beyond $1x10^8$ colony forming units (cfu) (Figure 19A). Infection of XIAP knockout mice ($XIAP^{-/-}$) with *S. flexneri* M90T ($1x10^7$ cfu) revealed a significant difference in sensitivity to infection compared to wildtype mice (Figure 19B). To further investigate the increased susceptibility of XIAP knockout mice to *S. flexneri* infection, we analysed the livers of infected XIAP knockout and wild type mice. Macroscopic as well as histological examinations revealed striking differences in their capacity to contain the inflammatory response to *S. flexneri* infection (Figure 19C and 19D). Whereas wildtype livers showed discrete granuloma-like areas of necrosis, enclosed and contained by a small rim of mononuclear cell aggregates, the livers of XIAP knockout mice showed disseminated necrotic lesions and broadly scattered inflammatory cells throughout the liver tissue (Figure 19D). These data reveal for the first time that XIAP knockout mice are profoundly impaired in their capacity to mount a directed inflammatory response to contain *S. flexneri* and as a result succumb to overwhelming bacterial infection.

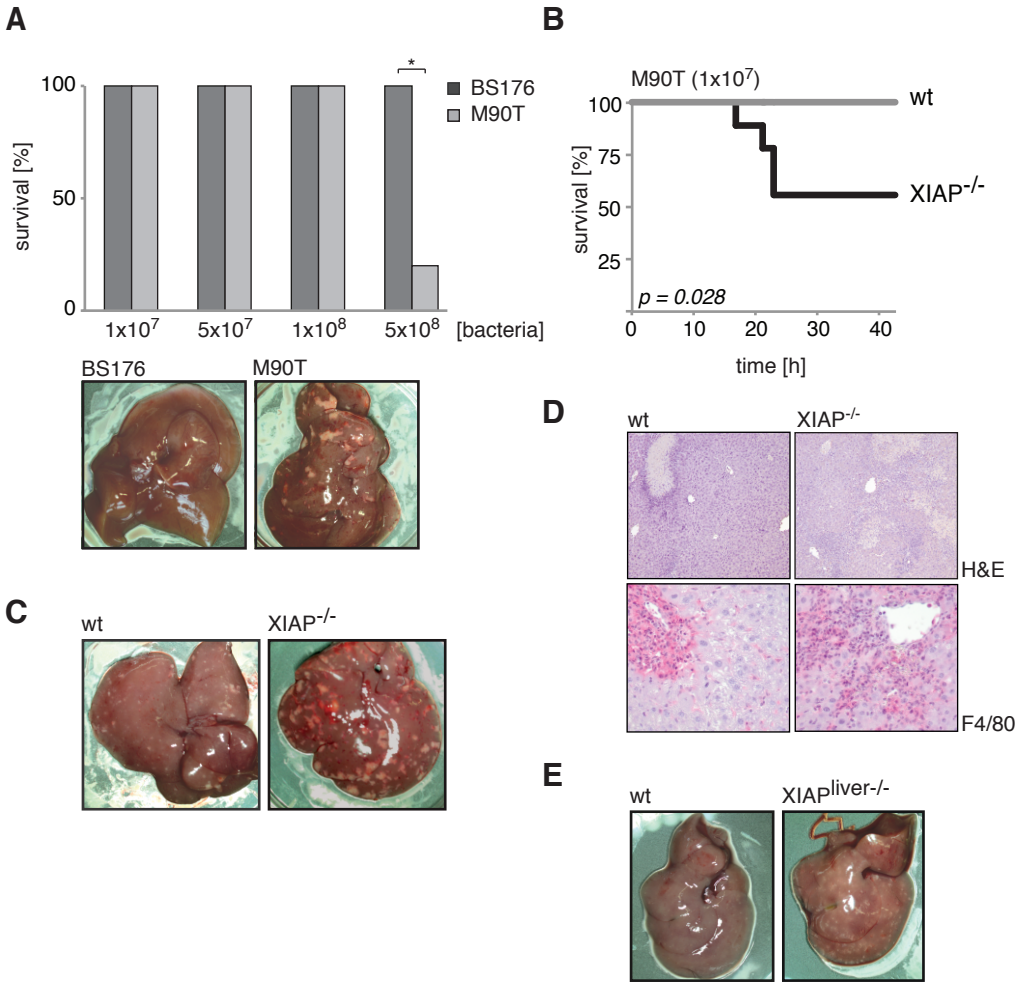

Figure 19. XIAP$^{-/-}$ and XIAP$^{liver-/-}$ mice are more susceptible to infection with *S. flexneri*.
(**A**) Wild type mice were *i.v.* infected with invasive *S. flexneri* M90T or non-invasive *S. flexneri* BS176 with the indicated cfu. Survival was monitored for 48 h. (n=5 in each group, *p<0.05)
(**B**) Kaplan-Meier curve of wild type (wt) and XIAP$^{-/-}$ mice infected with *S. flexneri* M90T (1x10^7 cfu). (XIAP$^{-/-}$: n=9; wt: n=9)
(**C**) Wild type mice and XIAP$^{-/-}$ mice were treated as in (B). Mice were sacrificed after 48 h and representative livers were analysed macroscopically with a SC 100 digital colour camera.
(**D**) Histological analysis of mouse liver at 48 h *p.i.*. Sections of infected liver were stained with hematoxylin and eosin or the indicated antibody, respectively.
(**E**) XIAP$^{fl/fl}$ and XIAP$^{liver-/-}$ mice were infected with *S. flexneri* M90T (1x10^7 cfu) as in (B). Mice were sacrificed after 24 h and livers were analysed macroscopically as in (C).

The systemic infection of mice with *S. flexneri* may not only lead to the bacterial colonisation of different organs and tissues but may similarly colonise immune cells and might affect the susceptibility towards *S. flexneri*. In order to specifically examine the role of XIAP in infected hepatocytes, a liver-specific XIAP knockout mouse was established. Liver-specific XIAP knockout mice (XIAP$^{liver-/-}$) and the corresponding wildtype mice (XIAP$^{fl/fl}$) were infected with *S. flexneri* M90T (1x10^7 cfu). Along with the XIAP complete-knockout data, the number and size of the necrotic liver lesions were much more severe in the liver specific XIAP$^{liver-/-}$ knockout mice than in the corresponding wildtype mice (XIAP$^{fl/fl}$) (Figure 19E). Interestingly, liver-specific XIAP deficiency did not culminate in increased mortality upon *S. flexneri* infection, suggesting that an overwhelming dysfunction of further tissues underlie the observed sensitivity of XIAP deficient mice to *S. flexneri* (data not shown). Nevertheless, these observations support the idea that XIAP is necessary for the cellular inflammatory signalling in response to *S. flexneri* infection, which in turn promotes an immune response to clear *S. flexneri* infection.

Finally, our *in vitro* analyses demonstrated that XIAP-mediated immune signalling is efficiently antagonised by the BID-mediated release of SMAC. Accordingly, in SMAC$^{-/-}$/OMI$^{+/-}$ knockout mice, XIAP-mediated inflammation should be unopposed and therefore mice should be more potent in clearing *S. flexneri* infection. Indeed, SMAC$^{-/-}$/OMI$^{+/-}$ knockout mice survived *S. flexneri* infection for a significantly longer period compared to wild type animals (Figure 20A, upper panel). Congruently, the livers of infected SMAC$^{-/-}$/OMI$^{+/-}$ knockout mice revealed fewer necrotic lesions than the corresponding wild type mice (Figure 20A lower panel), suggesting an efficient elimination of bacteria by non-antagonised XIAP-mediated immune signalling. Furthermore, BID knockout mice should similarly be unable to oppose XIAP-mediated inflammatory response against *S. flexneri* based on the lack of SMAC release. Indeed, unlike the corresponding wild type mice, BID knockout mice (BID$^{-/-}$)

appeared to be resistant to *S. flexneri*–induced infection (Figure 20B, upper panel) and develop fewer necrotic liver lesions compared to the corresponding wild type mice (Figure 20B, lower panel). Overall, these data underscore the pivotal role of XIAP in orchestrating the immune inflammatory response against *S. flexneri*.

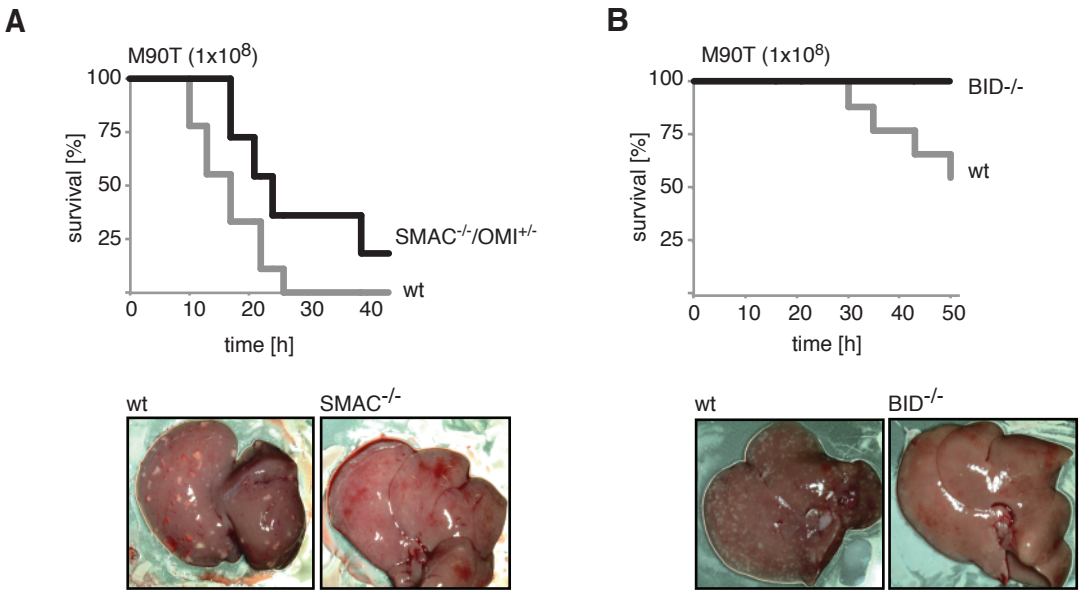

Figure 20. SMAC$^{-/-}$/OMI$^{+/-}$ and BID$^{-/-}$ mice show prolonged survival upon infection with *S.flexneri*.

(**A**) Kaplan Meier curve of wild type (wt) and SMAC$^{-/-}$/OMI$^{+/-}$ mice infected with *S. flexneri* M90T (1x10^{8}) (upper panel) and macroscopic analysis of the liver (lower panel). (SMAC$^{-/-}$/OMI$^{+/-}$: n=11; wt: n=9)
(**B**) Kaplan Meier curve of wild type (wt) and BID$^{-/-}$ mice infected with *S. flexneri* M90T (1x10^{8}) (upper panel) and macroscopic analysis of the liver (lower panel). (BID$^{-/-}$: n=9; wt: n=10)

In conclusion, these results demonstrate that BID-mediated SMAC-release facilitates the antagonisation of XIAP to escape the host immune response towards *S. flexneri.*

Discussion

In this work we describe a novel strategy of *Shigella* bacteria to evade the host cell immune response. We show that *S. flexneri* induces the calpain-mediated activation of BID, which triggers the BAX/BAK independent and selective release of SMAC and OMI from the mitochondrial inter-membrane space into the cytoplasm to antagonise the inflammatory mediator XIAP. In contrast to apoptotic stimuli, *S. flexneri*-induced mitochondrial membrane permeabilisation does not deplete the mitochondrial membrane potential, permitting Cyt c to be retained inside the mitochondria thus avoiding apoptotic cell death. This novel strategy ensures the host cell's survival and supports bacterial propagation.

XIAP is essential for the immune response against intracellular *S. flexneri*

Following infection of the intestinal epithelium by *S. flexneri,* an inflammatory response is initiated that involves intracellular sensing of bacterial peptidoglycans by NOD1, leading to activation of NF-κB and the release of inflammatory chemokines such as IL-8, that promote the infiltration of the mucosa with immune cells (Phalipon and Sansonetti, 2007). Recently, XIAP was identified as an essential component of the NOD signalling cascade (Krieg et al., 2009; Damgaard et al., 2012). However, the use of minimal peptidoglycan fragments to stimulate intracellular NOD signalling in these studies cannot fully reflect the complexity of bacterial infection.

Our study for the first time implicates XIAP in NOD1-mediated NF-κB signalling after infection with *S. flexneri* in both, cultured epithelial cells (Figure 6B and 7A) and in mouse models (Figure 19). Whole-body XIAP knockout mice showed significantly reduced survival in response to *S. flexneri* compared to wild type littermates and developed extensive liver damage characterised by severe necrotic lesions (Figure 19C). Previous studies have shown that XIAP knockout mice challenged with another Gram-negative bacterium *L. monocytogenes* also showed a drastically decreased survival rate due to a greater bacterial burden in the liver and reduced levels of inflammatory cytokines in bone marrow derived macrophages (Bauler et al., 2008). These authors proposed that XIAP played a critical role in modulating NF-κB activation and cytokine response in infected macrophages as effector cells of the innate immune response. They further show that the loss of inflammatory cytokine production in XIAP-deficient macrophages is thought to permit uncontrolled bacterial propagation in spleen and liver. However, our own data *in vitro*

showed that NF-κB activation was abolished in *S. flexneri*-infected epithelial cells when XIAP was down-regulated in HeLa cells or knocked-out in MEFs from XIAP deficient mice, suggesting that cell autonomous XIAP functions of epithelial cells could also be involved in the observed phenotype after *S. flexneri* infection. To investigate whether the liver damage observed in whole-body XIAP knock out mice could be due to the cell autonomous loss of XIAP function in the hepatocytes regardless of its functions in immune cells, we generated a novel hepatocyte-specific XIAP knockout mouse model. Remarkably, *S. flexneri* infection in this model reproduced the liver lesions observed in the whole-body XIAP knockout mice (Figure 19E). These findings highlight the pivotal cell autonomous function played by XIAP in epithelial cells during the inflammatory response towards *S. flexneri*. However, in view of the survival benefit of the hepatocyte-specific XIAP knockouts compared with whole-body knockout mice in response to *S. flexneri* infection (data not shown), it is evident that both, the cell autonomous functions of XIAP as well as its functions in innate immune cells are required for adequate antibacterial protection. Additional analyses of the cytokine production as well as the bacterial burden in the liver should substantiate our findings that XIAP is an important mediator of inflammation after *S. flexneri* infection in mice.

Other members of the IAP family, namely cIAP1 and cIAP2 have also been implicated in NOD signalling in response to bacterial infection and cIAP1 as well as cIAP2 deficient mice challenged with the NOD agonist MDP reportedly showed a diminished inflammatory response (Bertrand et al., 2009). However, in our preliminary analyses of cIAP1 and cIAP2 deficient MEFs we found no evidence that NF-κB activation was compromised in response to *S. flexneri* infection. cIAP1 and cIAP2 differ from XIAP with regard to their molecular functions and others have reported that they are not essential for NOD signalling (Damgaard et al., 2012). Given that the precise contribution of cIAP1 and cIAP2 in NOD signalling remains unclear in this study, we focussed on the function of XIAP in NOD signalling.

In order to investigate the role of XIAP in *S. flexneri* infection *in vivo*, it was important to establish an appropriate mouse model of infection. Unlike in humans, oral infection of adult mice with *S. flexneri* does not induce Shigellosis (Phalipon and Sansonetti, 2007). The reasons for this resistance remain unknown, however, new-born mice (4 days old) are susceptible to infection, which led Fernandez et al., 2003 to develop an oral new-born mouse infection model. Unfortunately, the new-born mouse model is extremely sensitive to age since 5-day-old new-borns are already refractory to infection. In this study, we therefore decided to use the intravenous infection mouse model that was initially described by Martino et al., 2005. In this model, injection of *S. flexneri* into the tail vein of recipient mice leads to

immediate micro-granuloma formation, augmented production of cytokine mRNA in the liver and in the blood and extensive hepatocyte necrosis (Martino et al., 2005). This is an important aspect, since Shigellosis in humans is also associated with cytokine production in the liver as well as abnormal liver function (Levine et al., 1974). A further advantage of the intravenous infection model is that administration of a relatively small number of bacteria is sufficient to induce severe inflammation in mice.

SMAC and OMI are selectively released from mitochondria

Numerous studies focussing on mitochondrial outer membrane permeabilisation have contributed to the current dogma that in apoptotic cells the release of mitochondrial proteins including SMAC, OMI and Cyt c from the *inter membrane space* (IMS) into the cytosol is a simultaneous process (Munoz-Pinedo et al., 2006; Youle and Strasser, 2008). In contrast, our data show that following *S. flexneri* infection, the selective release of soluble IMS proteins such as SMAC and OMI can be uncoupled from the simultaneous release of Cyt c (Figure 12A). This observation gives rise to further questions regarding the nature of the selective release mechanism. The current view holds that all IMS proteins are released through the same mitochondrial pore, which is formed by BAX and BAK molecules, even though the nature and compositions of this pore is still under investigation. BAX activation has been viewed as an immediate early event preceding mitochondrial outer membrane permeabilisation in apoptotic cells (Kashkar et al., 2005). In striking contrast to apoptotic stimuli, the release of SMAC and OMI in *S. flexneri*-infected cells was not accompanied by BAX activation (Figure 12A), indicating that *S. flexneri* induces mitochondrial outer membrane permeabilisation in a non-apoptotic manner. The selective release of SMAC and OMI therefore implies the existence of release mechanisms that are separate from the BAX/BAK pore. That such BAX/BAK independent release mechanisms in principle exist, is illustrated for example by the mitochondrial permeability transition pore that resides at contact sites between the mitochondrial outer and inner membranes and facilitates the release of IMS proteins from the mitochondria after Ca^{2+} accumulation (Henry-Mowatt et al., 2004). However, this event leads to complete rupture of the mitochondria, which is clearly different from the situation observed upon *S. flexneri* infection, where the mitochondria remain intact (Figure 13). Regarding the nature and selectivity of the putative BAX/BAK-independent release mechanism, our findings suggest that it does not simply operate by size exclusion since SMAC (21 kDa) and OMI (36 kDa) are both larger than Cyt c (14 kDa). An alternative possibility to consider is that Cyt c is in fact released into the cytoplasm along with SMAC and OMI but is subject to rapid proteasomal degradation explaining why apoptosis is

avoided as well as why Cyt c cannot be detected in cytosolic fractions. If this were the case, the level of Cyt c inside the mitochondria should decrease during the course of infection. However, we can discount this possibility based on our observation that i) Cyt c levels in isolated mitochondria remain unchanged during infection (Figure 12C) ii) immunofluorescent detection of Cyt c shows a mitochondrial rather than a diffuse cytoplasmic distribution (Figure 12B) iii) inhibition of the proteasome using bortezomib does not lead to Cyt c accumulation in the cytosolic fraction (data not shown).

Calpain-cleaved BID induces the selective release of SMAC

BID has been described as a pro-apoptotic protein that is activated upon caspase-8 cleavage (Li et al., 1998; Luo et al., 1998). The C-terminal BID cleavage product translocates to the mitochondria where it leads to mitochondrial membrane permeabilisation through the formation of the BAX/BAK pore that facilitates the simultaneous release of SMAC, OMI and Cyt c into the cytosol, culminating in apoptotic cell death. Several other proteases have also been shown to potently cleave BID, including calpain (Billen et al., 2008) - a Ca^{2+}-dependent cysteine protease, known for its function in cytoskeletal remodelling.

Intriguingly, we and others have shown that *S. flexneri* infection leads to activation of calpain (Bergounioux et al., 2012, Figure 17A). Importantly, our findings not only demonstrate that *S. flexneri* infection results in calpain-mediated BID cleavage (Figure 17B) – but that unlike caspase-8-cleaved BID, calpain-cleaved BID preferentially induces the release of SMAC but not of Cyt c from the mitochondria (Figure 18). Accordingly, calpain-cleaved BID differs from caspase-8-cleaved BID in its ability to selectively release SMAC without releasing Cyt c from the mitochondria, thus preventing apoptotic cell death. It has been shown previously, that caspase-8-cleaved recombinant BID activates BAX and triggers apoptotic cell death by inducing ultrastructural changes in the mitochondria including disruption of cristae junctions and opening of the cristae, where the majority of Cyt c is localised (Scorrano et al., 2002; D'Herde et al., 2000). The structural changes of the mitochondria at the onset of apoptosis are induced by the depletion of the mitochondrial membrane potential ($\Delta\Psi_m$) and are required for the efficient release of Cyt c into the cytosol (Gottlieb et al., 2003). Accordingly, Cyt c release in response to apoptotic stimulation can be avoided, given that the $\Delta\Psi_m$ is maintained for example by stimulating the respiratory chain with succinate (Gottlieb et al., 2003). Our data show, that in contrast to apoptotic stimuli, infection with *S. flexneri* does not involve the activation of BAX (Figure 12A) and the integrity of the mitochondrial structure as well as the $\Delta\Psi_m$ is maintained (Figure 13). Therefore, after *S. flexneri* infection the calpain-

cleaved BID fragment, does not induce collateral mitochondrial damage and therefore favours the retention of Cyt c inside the mitochondria, permitting infected cells to escape cell death and allow bacterial propagation; while SMAC/OMI are selectively released from the mitochondria to oppose the XIAP-mediated inflammatory response.

Our observation that calpain-mediated BID cleavage occurs after *S. flexneri* infection is supported by at least one previous report where calpain-mediated BID cleavage is described in the context of ischemic reperfusion (Chen et al., 2001). In contrast to our own observations, these authors claimed to observe the release of Cyt c from isolated mitochondria. Critically, however, Chen et al. failed to observe caspase activation calling the significance of their observed Cyt c release into question. That BID cleavage products can induce the selective release of SMAC from the mitochondria is supported by a report by Deng and colleagues who showed that activation of JNK following TNF stimulation leads to the BID cleavage product jBID, that induces the preferential release of SMAC from the mitochondria without inducing apoptosis (Deng et al., 2003), although the underlying mechanism and whether Cyt c is involved or not remains unclear. Even though it appears, that jBID shares the capacity for selective SMAC release with calpain cleaved BID; the size and therefore structural differences of the cleavage products might argue against a common mechanism.

Structural analyses showed that BID is highly similar to BAX or BAK (Suzuki et al., 2000; Moldoveanu et al., 2006). It is therefore assumed that after proteolytic activation, BID cleavage products are able to insert into the outer mitochondrial membrane in a BAX-like manner (Billen et al., 2008). Conceivably, calpain-cleaved BID itself could therefore form a pore in the mitochondrial outer membrane to facilitate the selective release of SMAC after *S. flexneri* infection. Given its smaller size compared to caspase-8-cleaved BID, it is possible that calpain-cleaved BID could undergo alternative folding and insertion into the mitochondrial outer membrane, which does not involve the activation of BAX and is therefore less potent to induce apoptosis. In order to investigate this hypothesis further, protein-membrane interaction studies with recombinant calpain cleaved BID could help to elucidate the insertion mechanisms.

Recently, BID has been implicated in the regulation of cellular pathways other than apoptosis including NOD signalling (Yeretssian et al., 2011). Specifically, BID was identified in a genome-wide RNA-interference screen as a component of the NOD-signalling cascade leading to NF-κB activation and the production of inflammatory cytokines. Accordingly, BID knockout mice were unable to mount a cytokine response towards NOD stimulation. This

study is controversial, however, since we and others have been unable to confirm the pro-inflammatory role of BID in NOD-signalling (Nachbur et al., 2012). In fact, our data show that BID cleavage after *S. flexneri* infection has anti-inflammatory functions caused by the selective release of SMAC, leading to XIAP inhibition and consequently interrupted NOD-signalling (Figure 18). In keeping with the proposed anti-inflammatory function of BID, BID knockout mice were less sensitive to *S. flexneri* infection compared to wild type mice, resulting in prolonged survival and fewer necrotic liver lesions (Figure 20B).

Therapeutic implications

Anti-virulence drugs targeting host proteins co-opted by bacterial pathogens are emerging as a potential alternative in addition to antibiotics, avoiding the intense selection pressure, which has led many bacterial strains to become resistant (Baron, 2010).

In this regard, our finding that *S. flexneri* employs the selective release of SMAC and OMI to interrupt the XIAP mediated anti-bacterial response has potential therapeutic implications. As a strategy to restore the pro-inflammatory activity of XIAP and boost the immune response towards *S. flexneri* infection, the XIAP antagonist SMAC represents an attractive therapeutic target. Indeed, we showed that when SMAC is down-regulated with specific siRNA in epithelial cells or is absent in MEFs derived from SMAC and OMI deficient mice, the inflammatory response is enhanced as illustrated by increased NF-κB activity (Figure 10). Furthermore we showed that, $SMAC^{-/-}/OMI^{+/-}$ mice were significantly more resistant to *S. flexneri* and developed fewer necrotic liver lesions compared to their wild type littermates (Figure 20A). These findings illustrate the critical function of unopposed XIAP activity in controlling bacterial infections and highlight SMAC as a promising therapeutic target for anti-virulence therapy. Although the search for SMAC inhibitors is in an early phase, due to the relatively low molecular mass and relatively small interaction surface with XIAP, screens for a “small molecule” inhibitor have already been initiated.

Another attractive therapeutic target identified in our study is calpain. Calpain inhibitors already exist and have been successfully used to target other bacterial functions such as phagosomal escape of *L. monocytogenes* thus blocking bacterial propagation (Lopez-Castejon et al., 2012). In the context of *S. flexneri* infection, drugs targeting calpain could prevent the BID-mediated release of SMAC and OMI in response to bacterial infection and therefore restore the XIAP-mediated immune responses to clear intracellular bacteria.

Conclusion

Recent evidence suggests that XIAP, besides its important function in apoptosis, also plays a critical role in innate immunity. Importantly, XIAP truncation or deletion in humans is associated with X-linked lymphoproliferative syndrome 2 (XLP type 2) a rare primary immunodeficiency syndrome associated with colitis (Rigaud et al., 2006; Pachlopnik Schmid et al., 2011), illustrating the important role of XIAP in immune regulation and its relevance for human inflammatory diseases.

Here we show that XIAP is also involved in regulating the immune response against bacterial infections. Our study sheds light on the intricate mechanisms employed by *S. flexneri* to efficiently down-regulate the host cell immune response towards bacterial infection. We demonstrate that *S. flexneri* hijacks mitochondrial signalling pathways to antagonise the inflammatory mediator XIAP by selectively releasing SMAC and OMI from the mitochondrial inter membrane space. SMAC and OMI release from mitochondria is dependent on BID, which is cleaved by *S. flexneri*-activated calpain. Unlike caspase-8-cleaved BID, calpain-cleaved BID does not induce Cyt c release, which in turn ensures host cell survival and thus permits bacterial propagation (Figure 21).

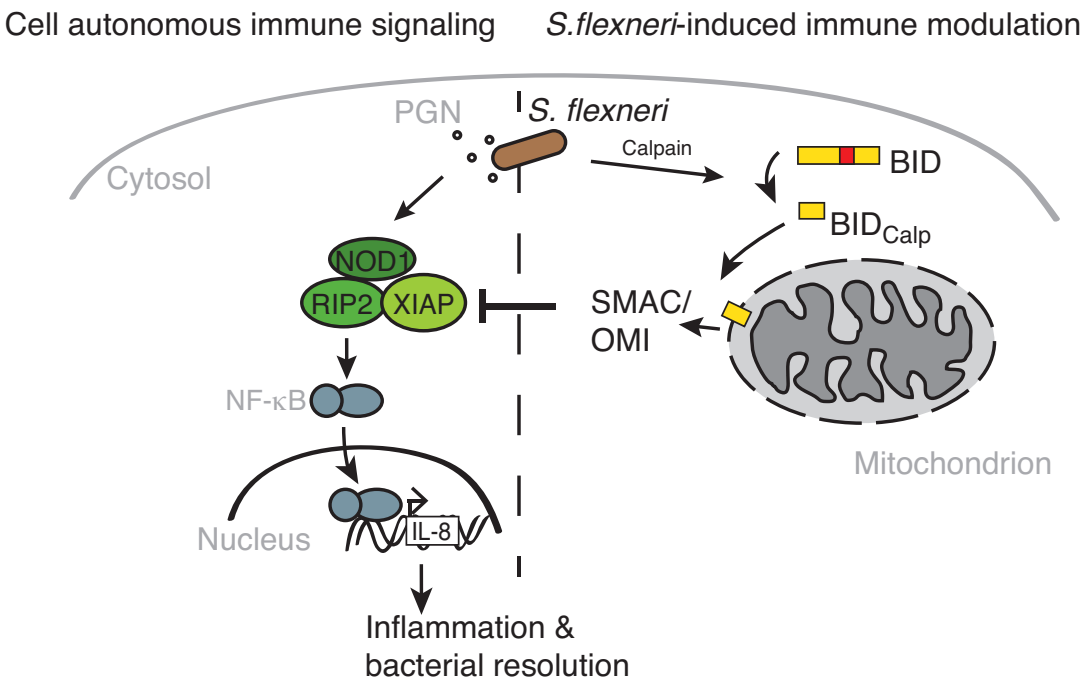

Figure 21. Proposed model of bacterial escape from XIAP-mediated immune response. Upon cytosolic appearance of *S. flexneri,* NOD1-signalling involving RIPK2 and XIAP is activated and promotes an inflammatory response (activation of NF-κB and IL-8 production) leading to bacterial resolution. However, *S. flexneri* evolved strategies to escape the innate immune defence by orchestrating a calpain- and BID-mediated, predominant release of mitochondrial SMAC and OMI to neutralise XIAP-mediated inflammatory signalling. PGN, peptidoglycan.

References

Ashida, H., Ogawa, M., Kim, M., Suzuki, S., Sanada, T., Punginelli, C., Mimuro, H., and Sasakawa, C. (2011). Shigella deploy multiple countermeasures against host innate immune responses. Current Opinion in Microbiology *14*, 16–23.

Baron, C. (2010). Antivirulence drugs to target bacterial secretion systems. Current Opinion in Microbiology *13*, 100–105.

Bauler, L.D., Duckett, C.S., and O'Riordan, M.X. (2008). XIAP regulates cytosol-specific innate immunity to Listeria infection. PLoS Pathogens *4*, e1000142.

Bergounioux, J., Elisee, R., Prunier, A.L., Donnadieu, F., Sperandio, B., Sansonetti, P., and Arbibe, L. (2012). Calpain Activation by the Shigella flexneri Effector VirA Regulates Key Steps in the Formation and Life of the Bacterium's Epithelial Niche. Cell Host & Microbe *11*, 240–252.

Bertrand, M.J., Doiron, K., Labbe, K., Korneluk, R.G., Barker, P.A., and Saleh, M. (2009). Cellular inhibitors of apoptosis cIAP1 and cIAP2 are required for innate immunity signaling by the pattern recognition receptors NOD1 and NOD2. Immunity *30*, 789–801.

Bertrand, M.J., Lippens, S., Staes, A., Gilbert, B., Roelandt, R., De Medts, J., Gevaert, K., Declercq, W., and Vandenabeele, P. (2011). cIAP1/2 are direct E3 ligases conjugating diverse types of ubiquitin chains to receptor interacting proteins kinases 1 to 4 (RIP1-4). PloS One *6*, e22356.

Billen, L.P., Shamas-Din, A., and Andrews, D.W. (2008). Bid: a Bax-like BH3 protein. Oncogene *27*, S93–104.

Birnbaum, M.J., Clem, R.J., and Miller, L.K. (1994). An apoptosis-inhibiting gene from a nuclear polyhedrosis virus encoding a polypeptide with Cys/His sequence motifs. Journal of Virology *68*, 2521–2528.

Chamaillard, M., Hashimoto, M., Horie, Y., Masumoto, J., Qiu, S., Saab, L., Ogura, Y., Kawasaki, A., Fukase, K., Kusumoto, S., et al. (2003). An essential role for NOD1 in host recognition of bacterial peptidoglycan containing diaminopimelic acid. Nature Immunology *4*, 702–707.

Chen, M., He, H., Zhan, S., Krajewski, S., Reed, J.C., and Gottlieb, R.A. (2001). Bid is cleaved by calpain to an active fragment in vitro and during myocardial ischemia/reperfusion. The Journal of Biological Chemistry *276*, 30724–30728.

Chipuk, J.E., Moldoveanu, T., Llambi, F., Parsons, M.J., and Green, D.R. (2010). The BCL-2 family reunion. Molecular Cell *37*, 299–310.

Clem, R.J., and Miller, L.K. (1994). Control of programmed cell death by the baculovirus genes p35 and iap. Molecular and Cellular Biology *14*, 5212–5222.

Clerc, P., and Sansonetti, P.J. (1987). Entry of Shigella flexneri into HeLa cells: evidence for directed phagocytosis involving actin polymerization and myosin accumulation. Infection and Immunity *55*, 2681–2688.

Cory, S., and Adams, J.M. (2002). The Bcl2 family: regulators of the cellular life-or-death switch. Nature Reviews. Cancer *2*, 647–656.

Crook, N.E., Clem, R.J., and Miller, L.K. (1993). An apoptosis-inhibiting baculovirus gene with a zinc finger-like motif. Journal of Virology *67*, 2168–2174.

D'Herde, K., De Prest, B., Mussche, S., Schotte, P., Beyaert, R., Coster, R. V, and Roels, F. (2000). Ultrastructural localization of cytochrome c in apoptosis demonstrates mitochondrial heterogeneity. Cell Death and Differentiation *7*, 331–337.

Damgaard, R.B., Nachbur, U., Yabal, M., Wong, W.W., Fiil, B.K., Kastirr, M., Rieser, E., Rickard, J.A., Bankovacki, A., Peschel, C., et al. (2012). The Ubiquitin Ligase XIAP Recruits LUBAC for NOD2 Signaling in Inflammation and Innate Immunity. Molecular Cell *46*, 746–758.

Deng, Y., Ren, X., Yang, L., Lin, Y., and Wu, X. (2003). A JNK-dependent pathway is required for TNFalpha-induced apoptosis. Cell *115*, 61–70.

Deveraux, Q.L., and Reed, J.C. (1999). IAP family proteins-suppressors of apoptosis. Genes & Development *13*, 239–252.

Deveraux, Q.L., Takahashi, R., Salvesen, G.S., and Reed, J.C. (1997). X-linked IAP is a direct inhibitor of cell-death proteases. Nature *388*, 300–304.

Dewson, G., and Kluck, R.M. (2009). Mechanisms by which Bak and Bax permeabilise mitochondria during apoptosis. Journal of Cell Science *122*, 2801–2808.

Dymecki, S.M. (1996). Flp recombinase promotes site-specific DNA recombination in embryonic stem cells and transgenic mice. PNAS *93*, 6191–6196.

Eckelman, B.P., and Salvesen, G.S. (2006). The human anti-apoptotic proteins cIAP1 and cIAP2 bind but do not inhibit caspases. The Journal of Biological Chemistry *281*, 3254–3260.

Fernandez, M.I., Thuizat, A., Pedron, T., Neutra, M., Phalipon, A., and Sansonetti, P.J. (2003). A newborn mouse model for the study of intestinal pathogenesis of shigellosis. Cellular Microbiology *5*, 481–491.

Fuentes-Prior, P., and Salvesen, G.S. (2004). The protein structures that shape caspase activity, specificity, activation and inhibition. The Biochemical Journal *384*, 201–232.

Galbán, S., and Duckett, C.S. (2010). XIAP as a ubiquitin ligase in cellular signaling. Cell Death and Differentiation *17*, 54–60.

Gesellchen, V., Kuttenkeuler, D., Steckel, M., Pelte, N., and Boutros, M. (2005). An RNA interference screen identifies Inhibitor of Apoptosis Protein 2 as a regulator of innate immune signalling in Drosophila. EMBO Rep *6*, 979–984.

Girardin, S.E., Tournebize, R., Mavris, M., Page, A.L., Li, X., Stark, G.R., Bertin, J., DiStefano, P.S., Yaniv, M., Sansonetti, P.J., et al. (2001). CARD4/Nod1 mediates NF-kappaB and JNK activation by invasive Shigella flexneri. EMBO Rep *2*, 736–742.

Girardin, S.E., Boneca, I.G., Carneiro, L.A., Antignac, A., Jehanno, M., Viala, J., Tedin, K., Taha, M.K., Labigne, A., Zahringer, U., et al. (2003). Nod1 detects a unique muropeptide from gram-negative bacterial peptidoglycan. Science *300*, 1584–1587.

Gottlieb, E., Armour, S.M., Harris, M.H., and Thompson, C.B. (2003). Mitochondrial membrane potential regulates matrix configuration and cytochrome c release during apoptosis. Cell Death and Differentiation *10*, 709–717.

Gyrd-Hansen, M., and Meier, P. (2010). IAPs: from caspase inhibitors to modulators of NF-kappaB, inflammation and cancer. Nature Reviews. Cancer *10*, 561–574.

Haubert, D., Gharib, N., Rivero, F., Wiegmann, K., Hösel, M., Krönke, M., and Kashkar, H. (2007). PtdIns(4,5)P-restricted plasma membrane localization of FAN is involved in TNF-induced actin reorganization. The EMBO Journal *26*, 3308–3321.

Henry-Mowatt, J., Dive, C., Martinou, J.-C., and James, D. (2004). Role of mitochondrial membrane permeabilization in apoptosis and cancer. Oncogene *23*, 2850–2860.

Hornig-Do, H.T., Gunther, G., Bust, M., Lehnartz, P., Bosio, A., and Wiesner, R.J. (2009). Isolation of functional pure mitochondria by superparamagnetic microbeads. Analytical Biochemistry *389*, 1–5.

Jost, P.J., Grabow, S., Gray, D., McKenzie, M.D., Nachbur, U., Huang, D.C.S., Bouillet, P., Thomas, H.E., Borner, C., Silke, J., et al. (2009). XIAP discriminates between type I and type II FAS-induced apoptosis. Nature *460*, 1035–1039.

Kashkar, H. (2010). X-linked inhibitor of apoptosis: a chemoresistance factor or a hollow promise. Clinical Cancer Research *16*, 4496–4502.

Kashkar, H., Wiegmann, K., Yazdanpanah, B., Haubert, D., and Kronke, M. (2005). Acid sphingomyelinase is indispensable for UV light-induced Bax conformational change at the mitochondrial membrane. The Journal of Biological Chemistry *280*, 20804–20813.

Kashkar, H., Seeger, J.M., Hombach, A., Deggerich, A., Yazdanpanah, B., Utermohlen, O., Heimlich, G., Abken, H., and Kronke, M. (2006). XIAP targeting sensitizes Hodgkin lymphoma cells for cytolytic T-cell attack. Blood *108*, 3434–3440.

Kashkar, H., Deggerich, A., Seeger, J.M., Yazdanpanah, B., Wiegmann, K., Haubert, D., Pongratz, C., and Kronke, M. (2007). NF-kappaB-independent down-regulation of XIAP by bortezomib sensitizes HL B cells against cytotoxic drugs. Blood *109*, 3982–3988.

Kaufmann, T., Tai, L., Ekert, P.G., Huang, D.C.S., Norris, F., Lindemann, R.K., Johnstone, R.W., Dixit, V.M., and Strasser, A. (2007). The BH3-only protein bid is dispensable for DNA damage- and replicative stress-induced apoptosis or cell-cycle arrest. Cell *129*, 423–433.

Kaufmann, T., Strasser, a, and Jost, P.J. (2012). Fas death receptor signalling: roles of Bid and XIAP. Cell Death and Differentiation *19*, 42–50.

Kellendonk, C., Opherk, C., Anlag, K., Schütz, G., and Tronche, F. (2000). Hepatocyte-specific expression of Cre recombinase. Genesis *26*, 151–153.

Kerr, J.F., Wyllie, A.H., and Currie, A.R. (1972). Apoptosis: a basic biological phenomenon with wide-ranging implications in tissue kinetics. British Journal of Cancer *26*, 239–257.

Krieg, A., Correa, R.G., Garrison, J.B., Le Negrate, G., Welsh, K., Huang, Z., Knoefel, W.T., and Reed, J.C. (2009). XIAP mediates NOD signaling via interaction with RIP2. PNAS *106*, 14524–14529.

Kufer, T.A., Banks, D.J., and Philpott, D.J. (2006). Innate immune sensing of microbes by Nod proteins. Annals Of The New York Academy Of Sciences *1072*, 19–27.

LaCasse, E.C., Mahoney, D.J., Cheung, H.H., Plenchette, S., Baird, S., and Korneluk, R.G. (2008). IAP-targeted therapies for cancer. Oncogene *27*, 6252–6275.

Lamkanfi, M., and Dixit, V.M. (2010). Manipulation of host cell death pathways during microbial infections. Cell Host & Microbe *8*, 44–54.

Levine, V., Overturf, G., and Mathies, A. (1974). Shigella dysenteriae type 1--severe dysentery and sepsis with hematologic, hepatic and renal complications. West J Med. *121*, 501–504.

Li, H., Zhu, H., Xu, C.J., and Yuan, J. (1998). Cleavage of BID by caspase 8 mediates the mitochondrial damage in the Fas pathway of apoptosis. Cell *94*, 491–501.

Li, P., Nijhawan, D., Budihardjo, I., Srinivasula, S.M., Ahmad, M., Alnemri, E.S., and Wang, X. (1997). Cytochrome c and dATP-dependent formation of Apaf-1/caspase-9 complex initiates an apoptotic protease cascade. Cell *91*, 479–489.

Lindsten, T., Ross, A.J., King, A., Zong, W.X., Rathmell, J.C., Shiels, H.A., Ulrich, E., Waymire, K.G., Mahar, P., Frauwirth, K., et al. (2000). The combined functions of proapoptotic Bcl-2 family members bak and bax are essential for normal development of multiple tissues. Molecular Cell *6*, 1389–1399.

Lopez-Castejon, G., Corbett, D., Goldrick, M., Roberts, I.S., and Brough, D. (2012). Inhibition of calpain blocks the phagosomal escape of Listeria monocytogenes. PloS One *7*, e35936.

Lu, M., Lin, S.C., Huang, Y., Kang, Y.J., Rich, R., Lo, Y.C., Myszka, D., Han, J., and Wu, H. (2007). XIAP induces NF-kappaB activation via the BIR1/TAB1 interaction and BIR1 dimerization. Molecular Cell *26*, 689–702.

Luo, X., Budihardjo, I., Zou, H., Slaughter, C., and Wang, X. (1998). Bid, a Bcl2 interacting protein, mediates cytochrome c release from mitochondria in response to activation of cell surface death receptors. Cell *94*, 481–490.

Mantis, N., Prevost, M.C., and Sansonetti, P. (1996). Analysis of epithelial cell stress response during infection by Shigella flexneri. Infection and Immunity *64*, 2474–2482.

Martino, M.C., Rossi, G., Tattoli, I., Martini, I., Chiavolini, D., Cortese, G., Pozzi, G., and Bernardini, M.L. (2005). Intravenous infection of virulent shigellae causes fulminant hepatitis in mice. Cellular Microbiology *7*, 115–127.

Martinou, J.C., and Youle, R.J. (2006). Which came first, the cytochrome c release or the mitochondrial fission? Cell Death and Differentiation *13*, 1291–1295.

Martins, L.M., Iaccarino, I., Tenev, T., Gschmeissner, S., Totty, N.F., Lemoine, N.R., Savopoulos, J., Gray, C.W., Creasy, C.L., Dingwall, C., et al. (2002). The serine protease Omi/HtrA2 regulates apoptosis by binding XIAP through a reaper-like motif. The Journal of Biological Chemistry *277*, 439–444.

Martins, L.M., Morrison, A., Klupsch, K., Fedele, V., Moisoi, N., Teismann, P., Abuin, A., Grau, E., Geppert, M., Livi, G.P., et al. (2004). Neuroprotective role of the Reaper-related serine protease HtrA2/Omi revealed by targeted deletion in mice. Molecular and Cellular Biology *24*, 9848–9862.

McKenzie, M.D., Carrington, E.M., Kaufmann, T., Strasser, A., Huang, D.C.S., Kay, T.W.H., Allison, J., and Thomas, H.E. (2008). Proapoptotic BH3-only protein Bid is essential for death receptor-induced apoptosis of pancreatic beta-cells. Diabetes *57*, 1284–1292.

Mizutani, Y., Nakanishi, H., Li, Y.N., Matsubara, H., Yamamoto, K., Sato, N., Shiraishi, T., Nakamura, T., Mikami, K., Okihara, K., et al. (2007). Overexpression of XIAP expression in renal cell carcinoma predicts a worse prognosis. International Journal of Oncology *30*, 919–925.

Moldoveanu, T., Liu, Q., Tocilj, A., Watson, M., Shore, G., and Gehring, K. (2006). The X-ray structure of a BAK homodimer reveals an inhibitory zinc binding site. Molecular Cell *24*, 677–688.

Munoz-Pinedo, C., Guio-Carrion, A., Goldstein, J.C., Fitzgerald, P., Newmeyer, D.D., and Green, D.R. (2006). Different mitochondrial intermembrane space proteins are released during apoptosis in a manner that is coordinately initiated but can vary in duration. PNAS *103*, 11573–11578.

Nachbur, U., Vince, J.E., O'Reilly, L. a, Strasser, A., and Silke, J. (2012). Is BID required for NOD signalling? Nature *488*, 4–6.

Pachlopnik Schmid, J., Canioni, D., Moshous, D., Touzot, F., Mahlaoui, N., Hauck, F., Kanegane, H., Lopez-Granados, E., Mejstrikova, E., Pellier, I., et al. (2011). Clinical similarities and differences of patients with X-linked lymphoproliferative syndrome type 1 (XLP-1/SAP deficiency) versus type 2 (XLP-2/XIAP deficiency). Blood *117*, 1522–1529.

Phalipon, A., and Sansonetti, P.J. (2007). Shigella's ways of manipulating the host intestinal innate and adaptive immune system: a tool box for survival? Immunol Cell Biol *85*, 119–129.

Philpott, D.J., Yamaoka, S., Israel, A., and Sansonetti, P.J. (2000). Invasive Shigella flexneri activates NF-kappa B through a lipopolysaccharide-dependent innate intracellular response and leads to IL-8 expression in epithelial cells. Journal of Immunology *165*, 903–914.

Prakash, H., Albrecht, M., Becker, D., Kuhlmann, T., and Rudel, T. (2010). Deficiency of XIAP leads to sensitization for Chlamydophila pneumoniae pulmonary infection and dysregulation of innate immune response in mice. The Journal of Biological Chemistry *285*, 20291–20302.

Rigaud, S., Fondaneche, M.C., Lambert, N., Pasquier, B., Mateo, V., Soulas, P., Galicier, L., Le Deist, F., Rieux-Laucat, F., Revy, P., et al. (2006). XIAP deficiency in humans causes an X-linked lymphoproliferative syndrome. Nature *444*, 110–114.

Salvesen, G.S., and Duckett, C.S. (2002). IAP proteins: blocking the road to death's door. Nature Reviews. Molecular Cell Biology *3*, 401–410.

Sattler, M., Liang, H., Nettesheim, D., Meadows, R.P., Harlan, J.E., Eberstadt, M., Yoon, H.S., Shuker, S.B., Chang, B.S., Minn, A.J., et al. (1997). Structure of Bcl-xL-Bak peptide complex: recognition between regulators of apoptosis. Science *275*, 983–986.

Schimmer, A.D., Dalili, S., Batey, R.A., and Riedl, S.J. (2006). Targeting XIAP for the treatment of malignancy. Cell Death and Differentiation *13*, 179–188.

Scorrano, L., Ashiya, M., Buttle, K., Weiler, S., Oakes, S.A., Mannella, C.A., and Korsmeyer, S.J. (2002). A distinct pathway remodels mitochondrial cristae and mobilizes cytochrome c during apoptosis. Developmental Cell *2*, 55–67.

Seeger, J.M., Brinkmann, K., Yazdanpanah, B., Haubert, D., Pongratz, C., Coutelle, O., Kronke, M., and Kashkar, H. (2010). Elevated XIAP expression alone does not confer chemoresistance. British Journal of Cancer *102*, 1717–1723.

Strasser, A., O'Connor, L., and Dixit, V.M. (2000). Apoptosis signaling. Annual Review of Biochemistry *69*, 217–245.

Suzuki, M., Youle, R.J., and Tjandra, N. (2000). Structure of Bax: coregulation of dimer formation and intracellular localization. Cell *103*, 645–654.

Tait, S.W., and Green, D.R. (2010). Mitochondria and cell death: outer membrane permeabilization and beyond. Nature Reviews. Molecular Cell Biology *11*, 621–632.

Tamm, I., Richter, S., Oltersdorf, D., Creutzig, U., Harbott, J., Scholz, F., Karawajew, L., Ludwig, W.-D., and Wuchter, C. (2004a). High expression levels of x-linked inhibitor of apoptosis protein and survivin correlate with poor overall survival in childhood de novo acute myeloid leukemia. Clinical Cancer Research *10*, 3737–3744.

Tamm, I., Richter, S., Scholz, F., Schmelz, K., Oltersdorf, D., Karawajew, L., Schoch, C., Haferlach, T., Ludwig, W.D., and Wuchter, C. (2004b). XIAP expression correlates with monocytic differentiation in adult de novo AML: impact on prognosis. The Hematology Journal *5*, 489–495.

Vandenabeele, P., and Bertrand, M.J. (2012). The role of the IAP E3 ubiquitin ligases in regulating pattern-recognition receptor signalling. Nature Reviews. Immunology.

Vaux, D.L., and Silke, J. (2005). IAPs, RINGs and ubiquitylation. Nature Reviews. Molecular Cell Biology *6*, 287–297.

Verhagen, A.M., Ekert, P.G., Pakusch, M., Silke, J., Connolly, L.M., Reid, G.E., Moritz, R.L., Simpson, R.J., and Vaux, D.L. (2000). Identification of DIABLO, a mammalian protein that promotes apoptosis by binding to and antagonizing IAP proteins. Cell *102*, 43–53.

Willis, S.N., Chen, L., Dewson, G., Wei, A., Naik, E., Fletcher, J.I., Adams, J.M., and Huang, D.C. (2005). Proapoptotic Bak is sequestered by Mcl-1 and Bcl-xL, but not Bcl-2, until displaced by BH3-only proteins. Genes & Development *19*, 1294–1305.

Yeretssian, G., Correa, R.G., Doiron, K., Fitzgerald, P., Dillon, C.P., Green, D.R., Reed, J.C., and Saleh, M. (2011). Non-apoptotic role of BID in inflammation and innate immunity. Nature *474*, 96–99.

Yin, X., Wang, K., Gross, A., Zhao, Y., Zinkel, S., Klocke, B., Roth, K.A., and Korsmeyer, S.J. (1999). Bid-deficient mice are resistant to Fas-induced hepatocellular apoptosis. Nature *400*, 2–7.

Youle, R.J., and Strasser, A. (2008). The BCL-2 protein family: opposing activities that mediate cell death. Nature Reviews. Molecular Cell Biology *9*, 47–59.

Zou, H., Li, Y., Liu, X., and Wang, X. (1999). An APAF-1.cytochrome c multimeric complex is a functional apoptosome that activates procaspase-9. The Journal of Biological Chemistry *274*, 11549–11556.

Appendix

Human BID sequence

5’-atggactgtgaggtcaacaacggttccagcctcagggatgagtgcatcacaaacctactggtgtttggcttcctccaaagctgttctgac

aacagcttccgcagagagctggacgcactgggccacgagctgccagtgctggctccccagtgggagggctacgatgagctgcagactg

Casp 8 ↓ Calpain ↓

atggcaaccgcagcagccactcccgcttgggaagaatagaggcagattctgaaagtcaagaagacatcatccggaatattgccaggcac

ctcgcccaggtcggggacagcatggaccgtagcatccctccgggcctggtgaacggcctggccctgcagctcaggaacaccagccgg

tcggaggaggaccggaacagggacctggccactgccctggagcagctgctgcaggcctaccctagagacatggagaaggagaagac

catgctggtgctggccctgctgctggccaagaaggtggccagtcacacgccgtccttgctccgtgatgtctttcacacaacagtgaattttatt

aaccagaacctacgcacctacgtgaggagcttagccagaaatgggatggactga-3’

Vector map

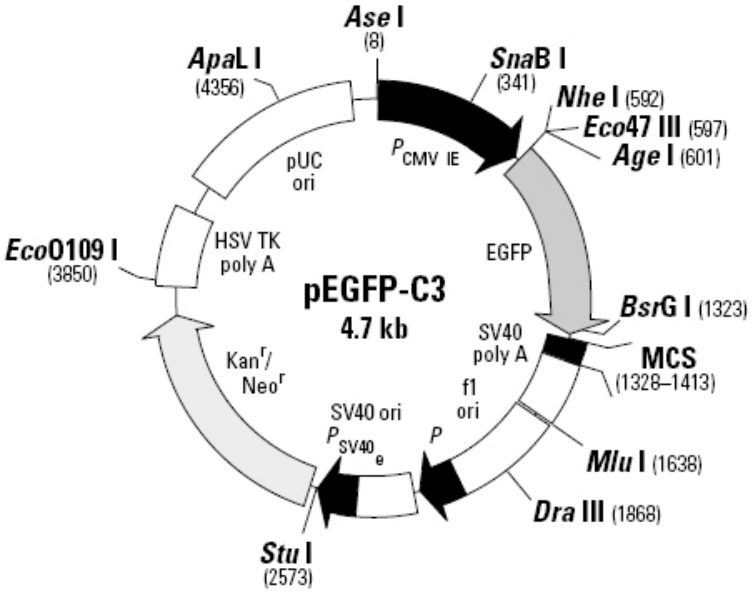

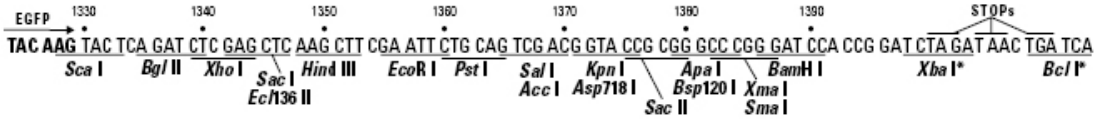

Erklärung

Ich versichere, dass ich die von mir vorgelegte Dissertation selbständig angefertigt, die benutzten Quellen und Hilfsmittel vollständig angegeben und die Stellen der Arbeit – einschließlich Tabellen, Karten und Abbildungen –, die anderen Werken im Wortlaut oder dem Sinn nach entnommen sind, in jedem Einzelfall als Entlehnung kenntlich gemacht habe; dass diese Dissertation noch keiner anderen Fakultät oder Universität zur Prüfung vorgelegen hat; dass sie noch nicht veröffentlicht worden ist sowie, dass ich eine solche Veröffentlichung vor Abschluss des Promotionsverfahrens nicht vornehmen werde. Die Bestimmungen dieser Promotionsordnung sind mir bekannt. Die von mir vorgelegte Dissertation ist von PD Dr. Hamid Kashkar, Prof. Dr. Elena Rugarli und Prof. Dr. Rudolf Wiesner betreut worden.